Title

Source and role of intestinally derived lysophosphatidic acid in dyslipidemia and atherosclerosis

Journal

Journal of Lipid Research, 56(4)

ISSN

0022-2275

Authors

Navab, Mohamad
Chattopadhyay, Arnab
Hough, Greg
et al.

Publication Date

2015-04-01

DOI

10.1194/jlr.m056614

Peer reviewed

Source and role of intestinally derived lysophosphatidic acid in dyslipidemia and atherosclerosis

Mohamad Navab,* Arnab Chattopadhyay,* Greg Hough,* David Meriwether,*,† Spencer I. Fogelman,* Alan C. Wagner,* Victor Grijalva,* Feng Su,§ G. M. Anantharamaiah, Lin H. Hwang,†† Kym F. Faull,†† Srinivasa T. Reddy,[1],*,†,†† and Alan M. Fogelman***

Department of Medicine,* Department of Molecular and Medical Pharmacology,† Department of Obstetrics and Gynecology,§ and Semel Institute for Neuroscience and Human Behavior,†† David Geffen School of Medicine at University of California, Los Angeles, Los Angeles, CA 90095-1736; and Department of Medicine,** University of Alabama at Birmingham, Birmingham, AL 35294

Abstract We previously reported that *i*) a Western diet increased levels of unsaturated lysophosphatidic acid (LPA) in small intestine and plasma of LDL receptor null (LDLR$^{-/-}$) mice, and *ii*) supplementing standard mouse chow with unsaturated (but not saturated) LPA produced dyslipidemia and inflammation. Here we report that supplementing chow with unsaturated (but not saturated) LPA resulted in aortic atherosclerosis, which was ameliorated by adding transgenic 6F tomatoes. Supplementing chow with lysophosphatidylcholine (LysoPC) 18:1 (but not LysoPC 18:0) resulted in dyslipidemia similar to that seen on adding LPA 18:1 to chow. PF8380 (a specific inhibitor of autotaxin) significantly ameliorated the LysoPC 18:1-induced dyslipidemia. Supplementing chow with LysoPC 18:1 dramatically increased the levels of unsaturated LPA species in small intestine, liver, and plasma, and the increase was significantly ameliorated by PF8380 indicating that the conversion of LysoPC 18:1 to LPA 18:1 was autotaxin dependent. Adding LysoPC 18:0 to chow increased levels of LPA 18:0 in small intestine, liver, and plasma but was not altered by PF8380 indicating that conversion of LysoPC 18:0 to LPA 18:0 was autotaxin independent. We conclude that *i*) intestinally derived unsaturated (but not saturated) LPA can cause atherosclerosis in LDLR$^{-/-}$ mice, and *ii*) autotaxin mediates the conversion of unsaturated (but not saturated) LysoPC to LPA.—Navab, M., A. Chattopadhyay, G. Hough, D. Meriwether, S. I. Fogelman, A. C. Wagner, V. Grijalva, F. Su, G. M. Anantharamaiah, L. H. Hwang, K. F. Faull, S. T. Reddy, and A. M. Fogelman. **Source and role of intestinally derived lysophosphatidic acid in dyslipidemia and atherosclerosis. *J. Lipid Res.* 2015.** 56: **871–887.**

Supplementary key words lysophosphatidylcholine • 6F peptide • apolipoprotein A-I mimetic peptides • genetically engineered tomato plants

This work was supported in part by US Public Health Service Grants HL-30568 and HL-34343; by the Laubisch, Castera, M. K. Grey Funds at University of California, Los Angeles; and by the Leducq Foundation. M.N., S.T.R., G.M.A., and A.M.F. are principals in Bruin Pharma, and A.M.F. is an officer in Bruin Pharma.

Manuscript received 8 December 2014 and in revised form 2 February 2015.

Published, JLR Papers in Press, February 2, 2015
DOI 10.1194/jlr.M056614

Our laboratories have been studying apoA-I mimetic peptides containing 18 amino acids for more than a decade (1). As a result of the success of the 4F peptide (peptide Ac-D-W-F-K-A-F-Y-D-K-V-A-E-K-F-K-E-A-F-NH_2) in multiple animal models of disease (2), clinical trials were undertaken with the 4F peptide that resulted in three reports (3–5). Two of these reports demonstrated efficacy, as measured by improvement in HDL anti-inflammatory properties, when the peptide was administered orally at high doses, despite achieving very low plasma peptide levels (3, 4). A third report described clinical trials in which low doses of peptide were administered intravenously or subcutaneously in order to achieve high plasma peptide levels with these low doses (5). Despite achieving high plasma peptide levels with these low doses, the third report was negative in terms of efficacy, as measured by the lack of improvement in HDL anti-inflammatory properties. The low doses used in the third report (5) had been tested in the first clinical trial, but these low doses were found not to be effective (3). To understand the differing clinical trial results, we returned to mouse studies. In the first of these mouse studies, the amount of peptide in the feces predicted efficacy as measured by improvement in HDL

Abbreviations: 4F peptide, peptide Ac-D-W-F-K-A-F-Y-D-K-V-A-E-K-F-K-E-A-F-NH_2; 6F peptide, peptide D-W-L-K-A-F-Y-D-K-F-F-E-K-F-K-E-F-F without blocked end groups; EV tomatoes, transgenic tomatoes expressing the control marker protein β-glucuronidase; *Ire1*, inositol-requiring enzyme 1; LDLR$^{-/-}$, LDL receptor null; LPA, lysophosphatidic acid; LPA 18:0, LPA with stearic acid at *sn*-1 and a hydroxyl group at *sn*-2; LPA 18:1, LPA with oleic acid at *sn*-1 and a hydroxyl group at *sn*-2; LPA 18:2, LPA with linoleic acid at *sn*-1 and a hydroxyl group at *sn*-2; LPA 20:4, LPA with arachidonic acid at *sn*-1 and a hydroxyl group at *sn*-2; *Lpcat3*, lysophosphatidyl acyltransferase 3; LysoPC, lysophosphatidylcholine; LysoPC 18:0, LysoPC with stearic acid at *sn*-1 and a hydroxyl group at *sn*-2; LysoPC 18:1, LysoPC with oleic acid at *sn*-1 and a hydroxyl group at *sn*-2; *Mtp*, microsomal triglyceride transfer protein; PLA_2, phospholipase A_2; PLA2G1B, phospholipase A_2 group 1B; PON, paraoxonase-1; SAA, serum amyloid A; Tg6F tomatoes, transgenic tomatoes expressing the 6F peptide; WD, Western diet.

[1]To whom correspondence should be addressed.
e-mail: sreddy@mednet.ucla.edu

anti-inflammatory properties and by decreases in plasma serum amyloid A (SAA) levels, but the plasma peptide levels did not predict efficacy (6). In the next study, the peptide concentration in the small intestine of LDL receptor null ($LDLR^{-/-}$) mice on a Western diet (WD) predicted efficacy as measured by the ability of the peptide to reduce tissue and plasma levels of proinflammatory oxidized metabolites of arachidonic and linoleic acids and by plasma SAA levels, but the plasma peptide levels again did not predict efficacy (7). In these mouse studies (6, 7), the dose required for efficacy was far above the highest dose tested in the human clinical trials that did not demonstrate efficacy (5). Additionally, we noted that the effective dose of these peptides tested in rabbits as measured by improvement in HDL anti-inflammatory properties, plasma SAA levels, and aortic atherosclerosis was also higher than the doses used in the third study (8). These studies demonstrated a significant correlation between the anti-inflammatory properties of HDL and plasma SAA levels ($P < 0.0001$), a significant correlation between the anti-inflammatory properties of HDL and aortic atherosclerosis ($P = 0.002$), and a significant correlation between plasma SAA levels and aortic atherosclerosis ($P = 0.0079$) (8). In normolipidemic monkeys, the dose required for efficacy as measured by improvement in HDL anti-inflammatory properties was also higher than the doses used in the third report (9, 10).

There were two reasons that a low dose of peptide was chosen for the clinical trials described in the third report, which did not demonstrate efficacy (5). First, because of the need to chemically synthesize the 4F peptides, the cost of production was very high. Second, there was a mistaken belief that the peptides act primarily in the plasma, and that the level of peptide in plasma was the critical success factor. Our studies subsequent to the third report (5) suggested that high doses of peptide (40–100 mg/kg/day) must be delivered to the small intestine in order to achieve efficacy (6, 7). The peptides used in the three reports of human clinical trials (3–5) contained blocked end groups, which can only be added by chemical synthesis. The cost of producing such chemically synthesized peptides for use at these high doses is prohibitive. Therefore, we searched for and found a peptide [peptide D-W-L-K-A-F-Y-D-K-F-F-E-K-F-K-E-F-F without blocked end groups (6F peptide)] that showed efficacy in mice as measured by plasma SAA levels and aortic atherosclerosis similar to the 4F peptides with blocked end groups (11). Peptides that require blocked end groups for efficacy cannot be expressed as a transgene. Because the 6F peptide did not require blocked end groups for efficacy, we expressed 6F peptide in transgenic tomatoes (Tg6F tomatoes). When freeze-dried and fed to $LDLR^{-/-}$ mice on WD at only 2.2% by weight of the diet, Tg6F was highly effective in ameliorating dyslipidemia and atherosclerosis (11). Feeding control tomatoes that were either wild type or made transgenic with the same vector, but containing a sequence for the expression of a control marker protein (β-glucuronidase) instead of 6F peptide, was not effective (11). The amelioration of dyslipidemia by Tg6F differed from earlier studies with the 4F peptide. The 4F peptide did not improve dyslipidemia but did improve HDL anti-inflammatory properties, plasma SAA levels, and atherosclerosis in animal models (1).

After feeding the mice Tg6F tomatoes, intact 6F peptide was found in the small intestine, but the levels of 6F peptide were below the level of detection in the plasma (11). In the course of investigating possible mechanisms of action, we found that Tg6F tomatoes (but not control tomatoes) significantly reduced lysophosphatidic acid (LPA) levels in the small intestine (11). Remarkably, the tissue content of unsaturated LPA in the small intestine significantly correlated with the extent of aortic atherosclerosis (11). LPA is emerging as an important signaling molecule in diverse biological processes and disease states (11–38), and its role in the pathogenesis of atherosclerosis has been emphasized in recent years (30–40).

There are two major pathways for the formation of LPA (23). The first pathway is illustrated by the example of phosphatidylcholine being acted on by phospholipase A_1 (PLA_1) or phospholipase A_2 (PLA_2) removing the acyl group from the *sn*-1 or *sn*-2 positions, respectively. Subsequently, lysophospholipase D (autotaxin) converts lysophosphatidylcholine (LysoPC) to LPA by removing choline from the *sn*-3 position of the lysophosphatidylcholine. The second pathway is illustrated by the example of phosphatidylcholine being acted on by phospholipase D to yield phosphatidic acid, or diacylglycerol being acted on by diacylglycerol kinase to yield phosphatidic acid. Phosphatidic acid can subsequently be acted upon by PLA_1 or PLA_2 to give LPA. A major pathway for the breakdown of LPA is by the action of LPPs (25, 41). LPA levels are largely determined by the balance between these pathways.

In a subsequent study, we found that feeding WD to $LDLR^{-/-}$ mice increased the levels of unsaturated (but not saturated) LPA in the small intestine compared with feeding the mice standard mouse chow even though WD contained less preformed LPA than did standard mouse chow (39). Adding unsaturated (but not saturated) LPA to standard mouse chow (which only contains 4% fat and very low levels of cholesterol) resulted in increased levels of unsaturated LPA in the small intestine that was similar to that seen on WD (39). Additionally, after supplementing standard mouse chow with unsaturated LPA, changes in gene expression in the small intestine, and changes in plasma SAA levels, total cholesterol levels, triglyceride levels, HDL-cholesterol levels, and fast-performance liquid chromatography lipoprotein profiles were similar to those seen on feeding the mice WD (39). Adding Tg6F (but not control tomatoes) to standard mouse chow supplemented with unsaturated LPA prevented the LPA-induced changes (39). While these studies (39) established the ability of intestinally derived unsaturated LPA to cause dyslipidemia and inflammation (i.e., increased levels of plasma SAA), these studies did not establish that the resulting dyslipidemia and inflammation would lead to atherosclerosis.

The studies reported here demonstrate that adding unsaturated (but not saturated LPA) to standard mouse chow produces aortic atherosclerosis similar to that seen on feeding $LDLR^{-/-}$ mice WD. Additionally, we also provide

evidence that is consistent with the hypothesis that intestinally derived unsaturated LPA is formed as a result of dietary unsaturated phosphatidylcholine being acted on in the small intestine by pancreatic phospholipase A_2 group 1B (PLA2G1B) to form LysoPC, which is then absorbed into enterocytes in the small intestine and converted to unsaturated LPA species by the action of autotaxin. Interestingly, our results suggest that intestinally derived saturated LysoPC is converted to saturated LPA by autotaxin-independent mechanisms and does not cause dyslipidemia. These studies also demonstrate that adding one species of unsaturated LysoPC or LPA to standard mouse chow can result in increased levels of other unsaturated LPA species by processes that appear to be quite complex.

MATERIALS AND METHODS

Materials

Tg6F tomatoes or transgenic tomatoes expressing the control marker protein β-glucuronidase (EV tomatoes) were constructed and grown at the Donald Danforth Plant Science Center in Saint Louis, MO; the seeds were removed, and the pulp and skin were quick frozen and shipped overnight frozen to the University of California, Los Angeles (UCLA) where the pulp and skins were freeze-dried, powdered, and stored as previously described (11, 39). LysoPC 16:0 (LysoPC with palmitic acid at *sn*-1 and a hydroxyl group at *sn*-2), 18:0 (LysoPC with stearic acid at *sn*-1 and a hydroxyl group at *sn*-2), and 18:1 (LysoPC with oleic acid at *sn*-1 and a hydroxyl group at *sn*-2) were purchased from Avanti Polar Lipids (Birmingham, AL; catalog numbers 855675, 855775, and 845875, respectively), as were LPA 18:0 (LPA with stearic acid at *sn*-1 and a hydroxyl group at *sn*-2) and LPA 18:1 (LPA with oleic acid at *sn*-1 and a hydroxyl group at *sn*-2) (catalog numbers 857128 and 857130, respectively). LPA 18:2 (LPA with linoleic acid at *sn*-1 and a hydroxyl group at *sn*-2) was purchased from Echelon Biosciences (Salt Lake City, UT; catalog number L0182). All of the purchased LysoPC and LPA species contained the acyl group at the *sn*-1 position and the hydroxyl group at the *sn*-2 position. A highly potent and specific oral small-molecule inhibitor of autotaxin (PF8380) was purchased from Sigma (Saint Louis, MO; catalog number SML0715-PF8380). Anti-α smooth muscle cell actin antibody (catalog number ab32575) was purchased from Abcam (Cambridge, UK). Rat anti-mouse CD68 antibody (catalog number MCA 1957) was purchased from Serotec (Kidlington, UK). All other materials were purchased from sources previously reported (11, 39).

Mice

$LDLR^{-/-}$ mice, originally purchased from Jackson Laboratories on a C57BL/6J background, were obtained from the breeding colony of the Department of Laboratory and Animal Medicine at the David Geffen School of Medicine at UCLA. Both male and female mice were used in these studies; the gender is stated in each figure legend. The mice were of different ages, which are also stated in each figure legend. The mice were maintained on standard mouse chow (Ralston Purina) before being switched to WD (Teklad, Harlan, catalog #TD88137). Freeze-dried and powdered Tg6F or control (EV) tomatoes were added to the diet at 2.2% by weight as previously described (11). LysoPC or LPA were mixed into chow as previously described (39), and the oral specific autotaxin inhibitor PF8380 (42, 43) was similarly added to chow. Prior to harvesting of organs, the mice were perfused under anesthesia to remove all blood (11, 39), and organs were harvested as described previously (11, 39). All mouse studies were approved by the Animal Research Committee at UCLA.

Assays

Determination of plasma lipids and paraoxonase-1 (PON) activity were performed as previously described (39). Quantification of aortic atherosclerosis and characterization of lesions were performed as described previously (10, 11, 44). Antibodies for detection of CD68 and anti-α smooth muscle cell actin were used in accordance with the suppliers' instructions. LPA was determined by LC/MS/MS as previously described (39) with the following modifications. Plasma (50 μl) and tissues (50–100 mg) were extracted using solid phase extraction cartridges (1 cc, 10 mg and 3 cc, 60 mg, Waters Oasis HLB, respectively) as previously described with addition of LPA 17:0 (Avanti Polar Lipids) as an internal standard (25 ng) to each sample (39). The extracted samples were dried under a nitrogen stream (30°C–37°C) and dissolved in methanol (75 μl), eluent A (25 μl, 10 mM ammonium acetate, pH 8.5) was added, samples were vortexed, and an aliquot (20 μl) was injected onto a reverse phase HPLC column (Luna C5, 5 μm, 150 × 2 mm with a guard column; Phenomenex, Torrance, CA) equilibrated in 65% eluent A and 35% eluent B (acetonitrile-methanol, 98:2, v/v) and eluted (200 μl/min) with an increasing concentration of eluent B (min/%B; 0/35, 0.5/35, 11.5/80, 12/35, 16/35). The effluent from the column was directed to an electrospray ion source (Agilent Jet Stream) connected to a triple quadrupole mass spectrometer (Agilent 6460, Santa Clara, CA) operating in the negative ion multiple reaction monitoring mode in which the intensities of specific parent→fragment ion transitions were recorded [LPA 20:4 (LPA with arachidonic acid, at *sn*-1 and a hydroxyl group at *sn*-2), 457→153, retention time 7.6 min; LPA 17:0, 423→153, internal standard, retention time 8.6 min; LPA 16:0, 409→153, retention time 7.8 min; LPA 18:0, 437→153, retention time 9.4 min; LPA 18:1, 435→153, retention time 8.3 min; LPA 18:2, 433→153, retention time 7.5 min] under previously optimized conditions (fragmentor voltage, collision energy, and cell accelerator voltages of 140, 14, and 7, respectively; Q1 and Q3 used with FWHM settings of Widest and Unit, respectively). With each batch of samples, a series of standard samples were prepared containing the LPAs of interest (0, 12.5, 25, 50, 100, 200, 400, and 800 ng analyte per ml) and the same amount of internal standard. Calibration curves were constructed from the data obtained with the standard samples (ordinate peak area LPA/internal standard, abscissa amount of LPA), and the amount of each LPA species in each sample was calculated by interpolation from the standard curve. Gene expression in the jejunum was performed by RT-quantitative PCR (qPCR) as described previously (39).

Statistical analysis

Statistical analyses were performed by ANOVA and by unpaired two-tailed *t*-test using GraphPad Prism version 5.03 (GraphPad Software, San Diego, CA). Statistical significance was considered achieved if $P < 0.05$.

RESULTS

Adding LPA 18:2 (but not LPA 18:0) to standard mouse chow causes dyslipidemia in $LDLR^{-/-}$ mice, confirming our previous studies

As previously reported (39), adding 1 μg per gram chow of unsaturated (but not saturated) LPA to standard mouse chow produced dyslipidemia that was qualitatively similar

to WD; that is, plasma total cholesterol and triglyceride levels were increased (**Fig. 1A**, B), and plasma HDL-cholesterol levels were decreased (Fig. 1C). Additionally, as shown in Fig. 1D, the dyslipidemia was accompanied by a decrease in the activity of the HDL-associated antioxidant enzyme PON.

Adding LPA 18:2 (but not 18:0) to standard mouse chow causes aortic atherosclerosis similar to that seen on feeding LDLR$^{-/-}$ mice WD

As shown in **Fig. 2**, adding 1 μg per gram chow of LPA 18:2 (but not LPA 18:0) to mouse chow produced aortic atherosclerosis by en face analysis that was similar to that seen on feeding LDLR$^{-/-}$ mice WD. Similar results were obtained when the area containing atherosclerotic lesions was determined in aortic root sections (**Fig. 3**). As shown in **Fig. 4**, macrophage lesion area was similar when the mice were fed WD or standard chow supplemented with LPA 18:2 (but not LPA 18:0). Interestingly, while the control tomatoes (EV tomatoes) were ineffective in reducing the percent of aorta with atherosclerosis (Fig. 2), or the area containing atherosclerotic lesions in aortic root sections (Fig. 3), addition of control tomatoes (EV tomatoes) significantly decreased macrophage area whether the mice were fed standard mouse chow supplemented with LPA 18:2 or WD (Fig. 4). However, in both cases the reduction in macrophage area was significantly greater with Tg6F compared with EV tomatoes (Fig. 4). As shown in **Fig. 5**, the reduction in α smooth muscle cell actin was similar whether the mice were fed standard mouse chow supplemented with LPA 18:2 or WD. In both cases, addition of Tg6F (but not EV) tomatoes significantly preserved aortic α smooth muscle cell actin content (Fig. 5).

Searching for natural sources of intestinally derived LPA

We previously reported that feeding LDLR$^{-/-}$ mice WD increased the levels of unsaturated (but not saturated) LPA in the small intestine (39), and that the levels of unsaturated LPA in the small intestine significantly correlated with the percent of aorta with atherosclerosis (11). We also reported that *i*) WD actually contains less preformed unsaturated LPA than standard mouse chow; *ii*) the amount of preformed LPA in the diet is significantly less than the 1 μg LPA per gram chow that we add in our experiments; and *iii*) based on the change in tissue LPA levels after adding 1 μg LPA per gram chow, it was evident that most of the LPA added to the standard mouse chow was either lost prior to reaching the small intestine or not

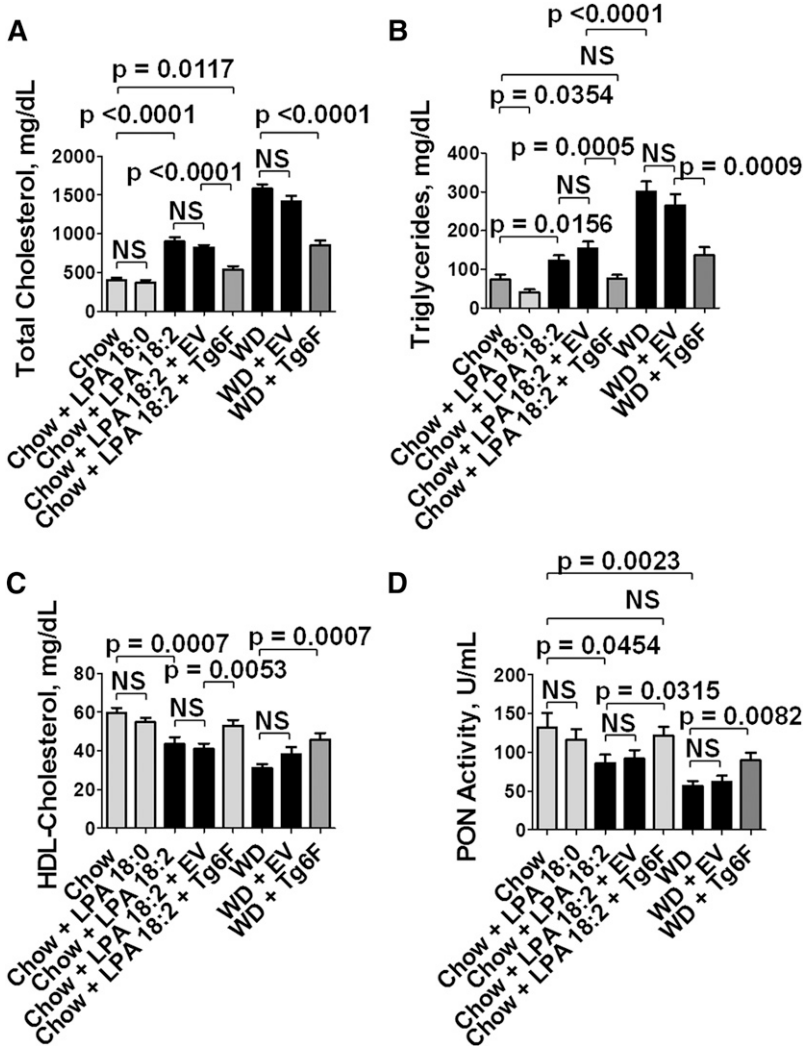

Fig. 1. Addition of unsaturated (but not saturated) LPA to standard mouse chow results in dyslipidemia and decreased PON activity. Female LDLR$^{-/-}$ mice 4–6 months of age (20–22 per group) were fed standard mouse chow, or standard mouse chow supplemented with 1 μg per gram chow of LPA 18:0 or LPA 18:2, or the mice were fed a WD. Some of the mice also received 2.2% by weight of freeze-dried EV tomatoes or Tg6F tomatoes. After 13 weeks, the mice were fasted overnight, and 20 mice from each group were bled to determine plasma lipids and PON activity as described in Materials and Methods. A: Plasma total cholesterol levels. B: Plasma triglyceride levels. C: Plasma HDL-cholesterol levels. D: Plasma PON activity. The data shown are mean ± SEM. NS, not significant.

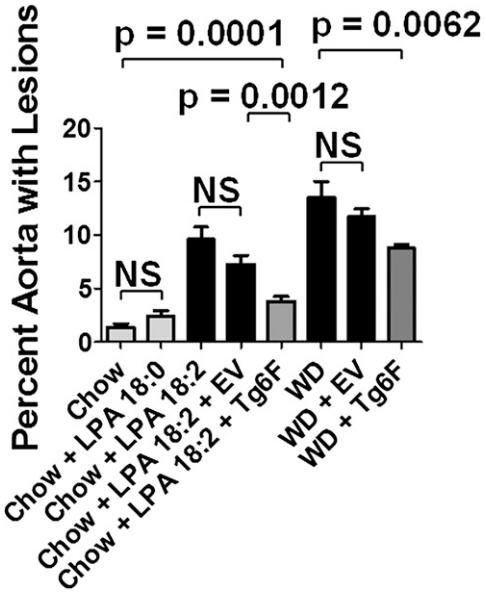

Fig. 2. Addition of unsaturated (but not saturated) LPA to standard mouse chow results in aortic atherosclerosis as determined by en face analysis. The percent of aorta with atherosclerosis as determined by en face analysis for the mice described in Fig. 1 was determined as described in Materials and Methods. The data shown are mean ± SEM. NS, not significant.

absorbed into the enterocytes of the small intestine (39). Thus, the natural source of small intestine LPA was not evident from our previous studies (39). We therefore sought

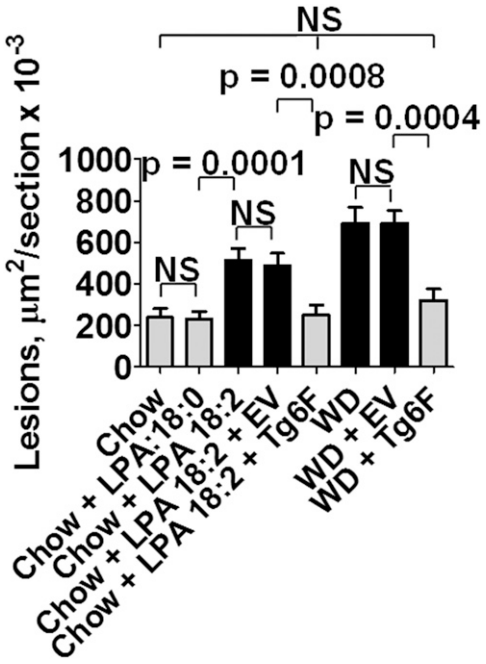

Fig. 3. Addition of unsaturated (but not saturated) LPA to standard mouse chow results in aortic atherosclerosis as determined by aortic root analysis. The area containing atherosclerotic lesions in aortic root sections of 15–19 randomly selected mice in each group described in Fig. 1 was determined as described in Materials and Methods. The data shown are mean ± SEM. NS, not significant. If chow is included in multiple comparisons, each comparison is to chow.

to identify a natural source for small intestine LPA, other than the minimal amounts of preformed LPA that are contained in the diets. One of the major pathways for the formation of LPA is through the action of autotaxin on LysoPC (23).

A major source of intestinal LysoPC is through the action of PLA2G1B (45–50). PLA2G1B is a pancreatic PLA_2 that hydrolyzes fatty acids at the *sn*-2 position of phospholipids in the lumen of the small intestine. The uptake of LysoPC formed by the action of PLA2G1B was reported to be very efficient and stimulated VLDL production (47). We hypothesized that LysoPC produced by the action of PLA2G1B on dietary unsaturated phospholipids might be a good substrate for the formation of unsaturated LPA in the enterocytes of the small intestine because *i*) LysoPC is readily absorbed into the enterocytes of the small intestine (49), and *ii*) autotaxin is highly expressed in the enterocytes of the small intestine (51).

Adding LysoPC 18:1 to standard mouse chow dose-dependently causes dyslipidemia and inflammation in LDLR$^{-/-}$ mice

In testing this hypothesis, we did not know how much LysoPC to add to standard mouse chow. Others have shown that a single intraperitoneal dose of 32 mg/kg of LysoPC into mice deficient in PLA2G1B restored functionality over a period of 1–4 h (47, 48). We assumed that adding LysoPC to standard mouse chow would require a much higher daily dose to deliver the needed concentration to the enterocytes of the small intestine over the many hours during which the mice eat. We decided that the best way to find the required dose was to determine the dose needed to increase plasma levels of total cholesterol, triglycerides, and SAA and decrease plasma HDL-cholesterol levels. As shown in **Fig. 6**, adding LysoPC 18:1 at doses ranging from 0.5 mg per gram of standard mouse chow to a dose of 4 mg per gram of standard mouse chow dose-dependently produced dyslipidemia and inflammation with the maximum response achieved at about 1 mg LysoPC 18:1 per gram standard mouse chow. In subsequent experiments, we used this dose (1 mg LysoPC per gram standard mouse chow). It should be noted that this dose of LysoPC is 1,000-fold higher than the dose of LPA (1 μg per gram standard mouse chow) that we routinely add to standard mouse chow. Our mice eat ~4 g of chow per day, so the dose of LysoPC administered was ~160 mg/kg taken over the course of 24 h (mostly during the night hours). It should also be noted that this dose of LysoPC 18:1 produced functional changes (dyslipidemia and plasma SAA levels) similar to that seen when 1 μg LPA 18:1 was added per gram standard mouse chow (160 μg/kg).

The dyslipidemia induced by supplementing standard mouse chow with LysoPC 18:1 is significantly ameliorated by adding a specific autotaxin inhibitor (PF8380)

As noted above, one of the major pathways for producing LPA is by the action of autotaxin on LysoPC (23). Therefore, we hypothesized that the dyslipidemia induced by unsaturated LysoPC (Fig. 6) might be due, at least in part, to unsaturated LPA formed by this pathway. To test

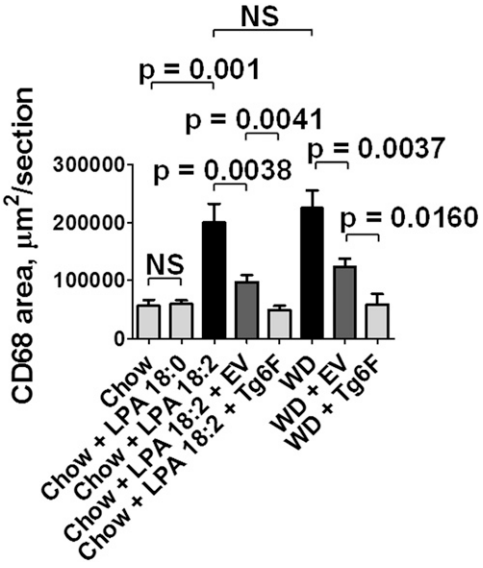

Fig. 4. Addition of unsaturated (but not saturated) LPA to standard mouse chow results in macrophage-rich aortic atherosclerosis. Aortic root sections from the mice described in Fig. 3 were randomly selected from 4 to 11 mice in each group for determination of macrophage area by staining for CD68 as described in Materials and Methods. The data shown are mean ± SEM. NS, not significant.

this hypothesis, we fed LDLR$^{-/-}$ mice chow supplemented with LysoPC 18:0 or 18:1 without or with the specific oral autotaxin inhibitor PF8380 that has been shown to inhibit autotaxin activity by >95% at a dose of 30 mg/kg (42, 43). As controls, we fed some of the mice standard mouse chow

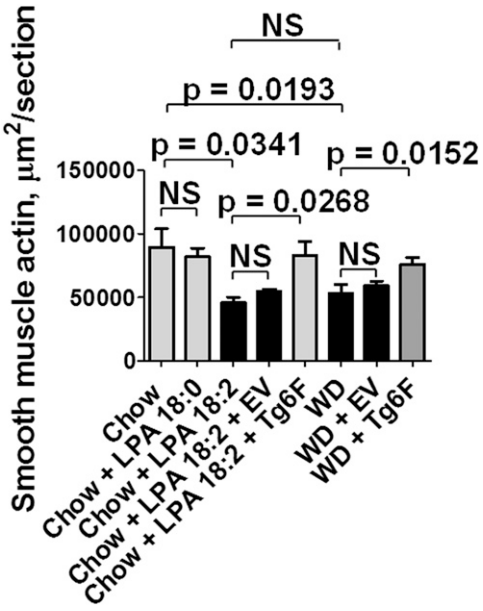

Fig. 5. Addition of unsaturated (but not saturated) LPA to mouse chow results in a significant reduction of aortic α smooth muscle cell actin. Aortic root sections from the mice described in Fig. 3 were randomly selected from 6 to 17 mice in each group for determination of aortic lesion α smooth muscle cell actin as described in Materials and Methods. The data shown are mean ± SEM. NS, not significant.

supplemented with LPA 18:1 without or with PF8380, or the mice were fed WD. As shown in **Fig. 7**, supplementing standard mouse chow with LysoPC 18:0 did not cause dyslipidemia, but supplementing standard mouse chow with LysoPC 18:1 produced dyslipidemia that was similar to that seen when the standard mouse chow was supplemented with LPA 18:1 or the mice were fed WD. Adding the specific oral autotaxin inhibitor PF8380 to the standard mouse chow supplemented with LysoPC 18:0 was without effect. In contrast, adding PF8380 to the standard mouse chow supplemented with LysoPC 18:1 significantly ameliorated the dyslipidemia and improved PON activity. Interestingly, adding PF8380 to standard mouse chow supplemented with LPA 18:1 significantly ameliorated plasma total cholesterol levels (Fig. 7A) but did not significantly alter plasma triglyceride levels (Fig. 7B) or HDL-cholesterol levels (Fig. 7C) or PON activity (Fig. 7D).

Adding LysoPC 18:0 or LysoPC 18:1 or LPA 18:1 to standard mouse chow produces complex changes in the levels of LPA species in the tissue of the jejunum

To directly test whether LysoPC is converted to LPA in the tissue of the jejunum, we added LysoPC 18:0 or LysoPC 18:1 at 1 mg per gram chow ± the autotaxin inhibitor PF8380 at 30 mg/kg to standard mouse chow. Controls included standard mouse chow alone or LPA 18:1 added to standard mouse chow at 1 μg per gram chow ± the autotaxin inhibitor PF8380 at 30 mg/kg, or the mice were fed WD. After 2 weeks on these diets, the mice were bled to obtain plasma, and after they were perfused to remove all remaining blood from the tissues, the levels of various LPA species in the tissue of the jejunum were determined by LC/MS/MS.

The levels of LPA 16:0 were not significantly altered in the jejunum by any of the diets administered (**Fig. 8A**). In contrast, the levels of LPA 18:0 in the jejunum were significantly increased on feeding LysoPC 18:0, and the levels were not significantly different if the autotaxin inhibitor PF8380 was included in the diet indicating that the conversion of LysoPC 18:0 to LPA 18:0 in the tissue of the jejunum was likely by autotaxin-independent pathways (Fig. 8B). Feeding the LDLR$^{-/-}$ mice either LysoPC 18:1 or LPA 18:1 did not significantly change the levels of LPA 18:0 in the tissue of the jejunum, and PF8380 was without effect (Fig. 8B) indicating that *i*) saturated LysoPC is not formed from unsaturated LysoPC or from unsaturated LPA under these conditions; and *ii*) inhibiting autotaxin does not affect the levels of LysoPC 18:0 in the tissue of the jejunum, regardless of the species of LysoPC or LPA added to the diet. Feeding WD modestly but significantly increased the levels of LPA 18:0 in the jejunum (Fig. 8B).

Feeding the LDLR$^{-/-}$ mice LysoPC 18:0 ± the autotaxin inhibitor PF8380 did not significantly alter the levels of LPA 18:1 in the tissue of the jejunum (Fig. 8C). However, feeding LysoPC 18:1 significantly increased levels of LPA 18:1 in the jejunum, and this was significantly ameliorated by PF8380, which is consistent with an autotaxin-dependent mechanism mediating the conversion of LysoPC 18:1 to LPA 18:1 (Fig. 8C). Feeding LPA 18:1 modestly,

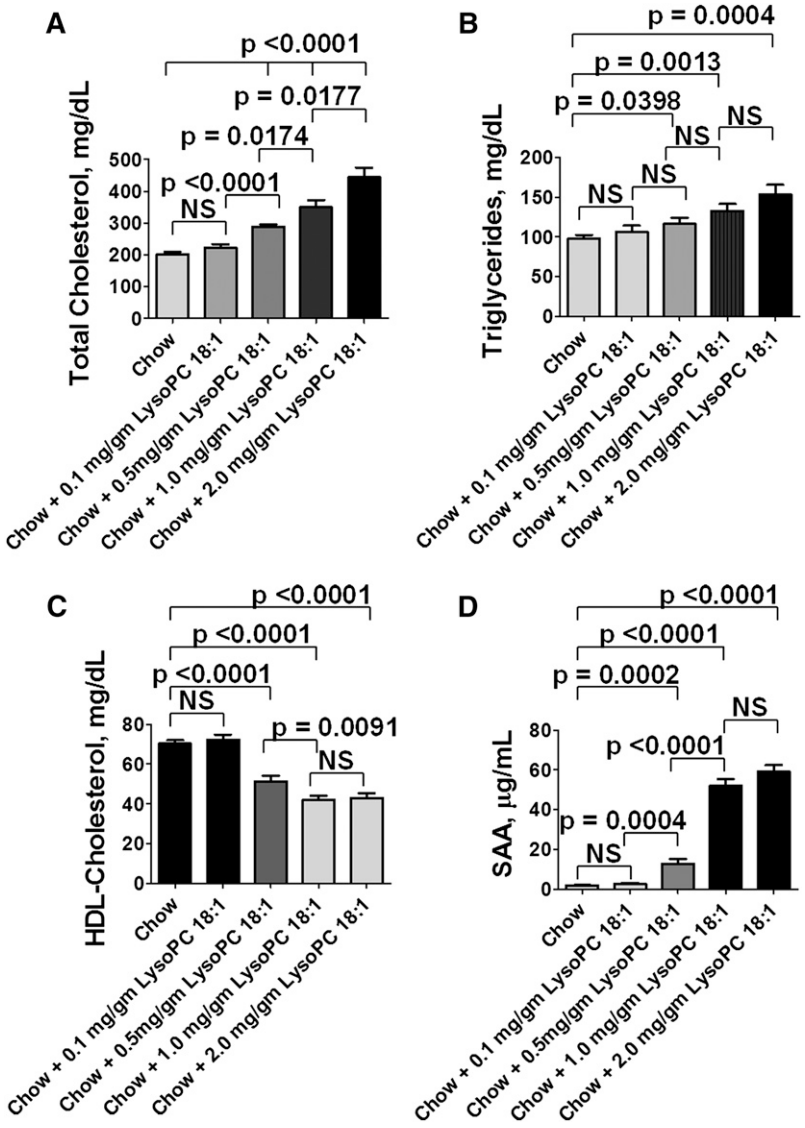

Fig. 6. Adding LysoPC 18:1 to standard mouse chow dose-dependently produces dyslipidemia and inflammation in LDLR$^{-/-}$ mice. Female LDLR$^{-/-}$ mice 4–6 months of age (20 per group) were fed mouse chow or mouse chow supplemented with LysoPC 18:1 at a dose of 0.1 mg/g chow, 0.5 mg/g chow, 1.0 mg/g chow, or 2 mg/g chow. After 2 weeks, the mice were fasted overnight, and blood was collected for determination of plasma lipids and SAA as described in Materials and Methods. A: Plasma total cholesterol levels. B: Plasma triglyceride levels. C: Plasma HDL-cholesterol levels. D: Plasma SAA levels. The data shown are mean ± SEM. NS, not significant. If chow is included in multiple comparisons, each comparison is to chow.

but significantly increased the levels of LPA 18:1 in the jejunum and was not altered by PF8380 (Fig. 8C). It is interesting that feeding LPA 18:1 was much less effective in raising the levels of LPA 18:1 in the tissue of the jejunum compared with feeding the mice LysoPC 18:1. Feeding WD modestly, but significantly increased the levels of LPA 18:1 in the jejunum (Fig. 8C).

The levels of LPA 18:2 in the jejunum were not altered by feeding LysoPC 18:0 ± the autotaxin inhibitor PF8380 (Fig. 8D). However, levels of LPA 18:2 in the tissue of the jejunum were significantly increased by feeding LysoPC 18:1, and the increase was significantly ameliorated by PF8380 consistent with an autotaxin-dependent mechanism (Fig. 8D). Feeding the LDLR$^{-/-}$ mice LPA 18:1 significantly increased the levels of LPA 18:2 in the jejunum, and the levels were not altered by inhibiting autotaxin with PF8380 (Fig. 8D). It is interesting that feeding LPA 18:1 was much more effective in raising the levels of LPA 18:2 in the tissue of the jejunum compared with feeding the mice LysoPC 18:1. This is just the opposite of the case for LPA 18:1 levels in the tissue of the jejunum where LysoPC 18:1 was much more effective in increasing the tissue levels of LPA 18:1 (Fig. 8C). WD also significantly increased the levels of LPA 18:2 in the tissue of the jejunum (Fig. 8D).

Feeding the LDLR$^{-/-}$ mice LysoPC 18:0 did not significantly alter the levels of LPA 20:4 in the tissue of the jejunum (Fig. 8E). However, adding PF8380 to chow supplemented with LysoPC 18:0 very slightly, but significantly increased the levels of LPA 20:4 in the tissue of the jejunum (Fig. 8E). Feeding LysoPC 18:1 significantly increased the levels of LPA 20:4 in the jejunum, and this was significantly decreased by PF8380 consistent with an autotaxin-dependent mechanism (Fig. 8E). Adding LPA 18:1 to the standard mouse chow slightly, but significantly increased the levels of LPA 20:4 in the tissue of the jejunum, and this was not significantly altered by inhibiting autotaxin with PF8380 (Fig. 8E). It is interesting that LysoPC 18:1 was significantly more effective in increasing the levels of LPA 20:4 in the tissue of the jejunum compared with feeding the mice LPA 18:1 (Fig. 8E). Thus, feeding LysoPC 18:1 was much more effective in increasing the levels of both LPA 18:1 and LPA 20:4 in the tissue of the jejunum

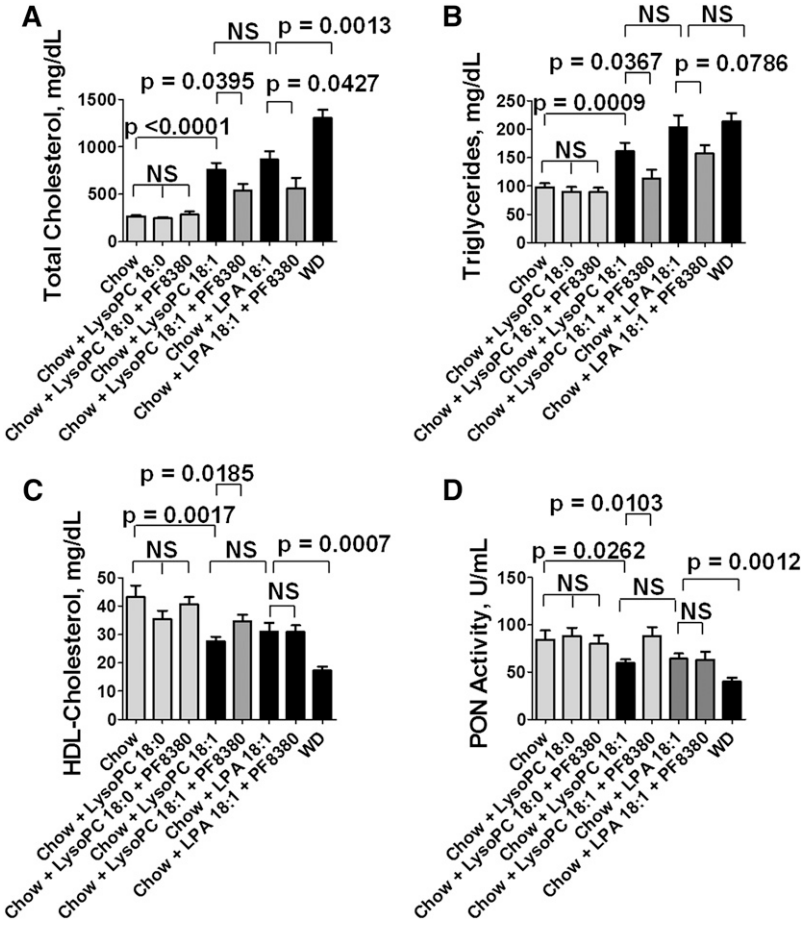

Fig. 7. The dyslipidemia induced by supplementing standard mouse chow with LysoPC 18:1 is significantly ameliorated by adding a specific autotaxin inhibitor (PF8380). Male LDLR$^{-/-}$ mice 9–10 months of age (20 per group) were fed standard mouse chow or standard mouse chow plus LysoPC 18:0 or LysoPC 18:1 at 1 mg per gram chow without or with 30 mg/kg of the specific oral autotaxin inhibitor PF8380, or the mice were fed standard mouse chow supplemented with LPA 18:1 at 1 μg per gram chow without or with 30 mg/kg of PF8380, or the mice were fed a WD. After 2 weeks, the mice were fasted overnight, bled, and plasma lipids and PON activity were determined as described in Materials and Methods. A: Plasma total cholesterol levels. B: Plasma triglyceride levels. C: HDL-cholesterol levels. D: PON activity. The data shown are mean ± SEM. NS, not significant. If chow is included in multiple comparisons, each comparison is to chow.

compared with feeding LPA 18:1, but feeding the mice LPA 18:1 was more effective in increasing the tissue levels of LPA 18:2 compared with feeding the mice LysoPC 18:1. Feeding WD did not significantly increase the levels of LPA 20:4 in the tissue of the jejunum (Fig. 8E).

Adding LysoPC 18:0 or LysoPC 18:1 or LPA 18:1 to standard mouse chow produces directional changes in the liver and plasma similar to those seen in the jejunum for most LPA species

We thought it was important to determine whether similar changes were observed in other tissues. We chose to examine the liver because of its major role in regulating plasma lipoprotein levels; we also chose to examine plasma because of its role in reflecting and modulating many different tissues. Because blood was collected for plasma prior to the mice being thoroughly perfused to remove all remaining blood from tissues before harvesting the organs, we felt that it was valid to compare the levels of LPA in the plasma to those seen in jejunum and liver.

As shown in **Figs. 9** and **10**, similar to the case for the jejunum feeding the mice LysoPC 18:0 significantly increased the levels of LPA 18:0 in an autotaxin-independent manner in liver and plasma but did not alter levels of LPA 18:1, LPA 18:2, or LPA 20:4.

Similar to the case for the jejunum, feeding LysoPC 18:1 increased levels of LPA 18:1 and LPA 20:4 in liver and plasma much more than when the mice were fed LPA 18:1, and the LysoPC 18:1-mediated increases were autotaxin dependent (Figs. 9 and 10).

Similar to the case for the jejunum, feeding the mice LPA 18:1 increased levels of LPA 18:2 in liver and plasma much more than when the mice were fed LysoPC 18:1, and the LPA 18:1-mediated increases were autotaxin independent (Figs. 9 and 10).

Differences in the responses of the jejunum (Fig. 8), liver (Fig. 9), and plasma (Fig. 10) included the following: *1*) an increase in LPA 16:0 levels in liver on feeding WD, but not in jejunum or plasma; *2*) decreased levels of LPA 18:0 in liver on feeding LPA 18:1, but not in jejunum or plasma; *3*) increased levels of LPA 18:0 in jejunum and plasma on feeding WD, but not in liver; *4*) increased levels of LPA 18:0 in plasma on feeding LysoPC 18:1, but not in jejunum or liver; and *5*) increased levels of LPA 20:4 in plasma on feeding WD, but not in jejunum or liver.

Directly comparing changes in jejunum, liver, and plasma

To be able to directly compare changes in jejunum with those in liver and plasma, the average value for mice receiving standard mouse chow without supplements was calculated for each LPA species in each tissue in the mice described in Figs. 8–10. Subsequently, the value for each mouse receiving a diet other than standard mouse chow alone (except for data from mice receiving PF8380, which were excluded from this analysis) was compared with this average value to obtain the fold-change compared with

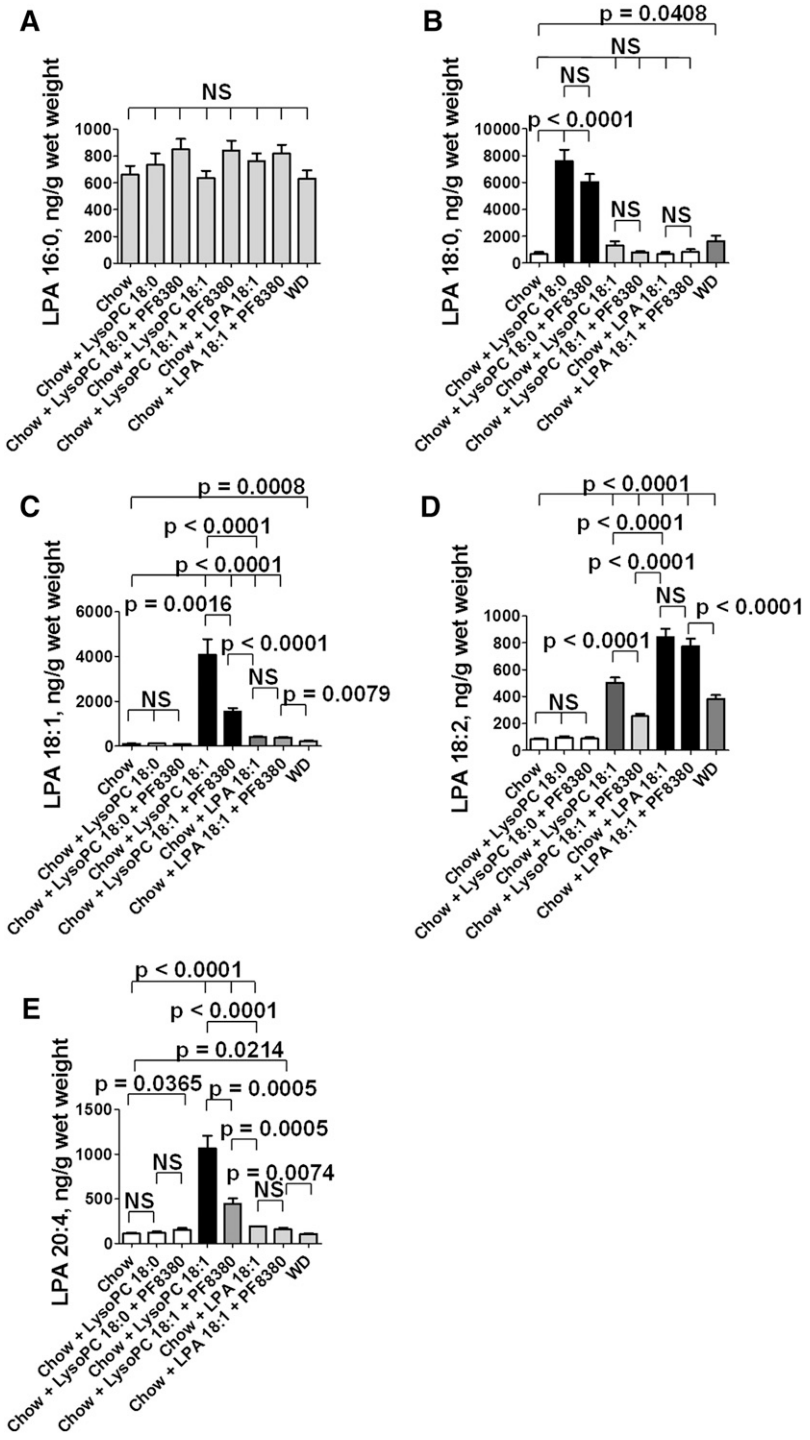

Fig. 8. Adding LysoPC 18:0 or LysoPC 18:1 or LPA 18:1 to standard mouse chow produces complex changes in the levels of LPA species in the tissue of the jejunum. Male LDLR$^{-/-}$ mice 5–7 months of age (20 per group) were fed standard mouse chow or standard mouse chow plus LysoPC 18:0 or LysoPC 18:1 at 1 mg per gram chow without or with 30 mg/kg of the specific oral autotaxin inhibitor PF8380, or the mice were fed standard mouse chow supplemented with LPA 18:1 at 1 μg per gram chow without or with 30 mg/kg of PF8380, or the mice were fed a WD. After 2 weeks, the mice were fasted overnight; under anesthesia, the mice were bled and perfused to remove all blood as described in Materials and Methods; and the jejunum was harvested and processed to determine LPA tissue levels as described in Materials and Methods. A: The levels of LPA 16:0. B: The levels of LPA 18:0. C: The levels of LPA 18:1. D: The levels of LPA 18:2. E: The levels of LPA 20:4. The data shown are mean ± SEM. NS, not significant. If chow is included in multiple comparisons, each comparison is to chow.

standard mouse chow alone. The results are shown in **Fig. 11A**–E for each LPA species measured.

The fold-change compared with standard mouse chow alone for LPA 16:0 was modest for all, but greatest in the liver of mice receiving WD (Fig. 11A). The greatest change compared with standard mouse chow alone for LPA 18:0 was in the jejunum of mice receiving LysoPC 18:0 where the fold-increase was 11.1 ± 1.2 (mean ± SEM) (Fig. 11B). The greatest change compared with standard mouse chow alone for LPA 18:1 was in the jejunum of mice receiving LysoPC 18:1 where the fold-increase was 38.6 ± 6.5 (Fig. 11C). The greatest fold-change for LPA 18:2 was in the jejunum and liver of mice receiving LPA 18:1 where the fold-increase was 10 ± 1 and 11 ± 2, respectively (Fig. 11D).

The greatest fold-change compared with standard mouse chow alone for LPA 20:4 occurred in plasma of mice receiving LysoPC 18:1 with a fold-increase of 24.2 ± 2.7 (Fig. 11E).

Adding unsaturated (but not saturated) LPA to standard mouse chow increases gene expression in the jejunum to favor the remodeling of phospholipid fatty acids

One of the striking findings in the data presented above is that adding LysoPC 18:1 to standard mouse chow induced

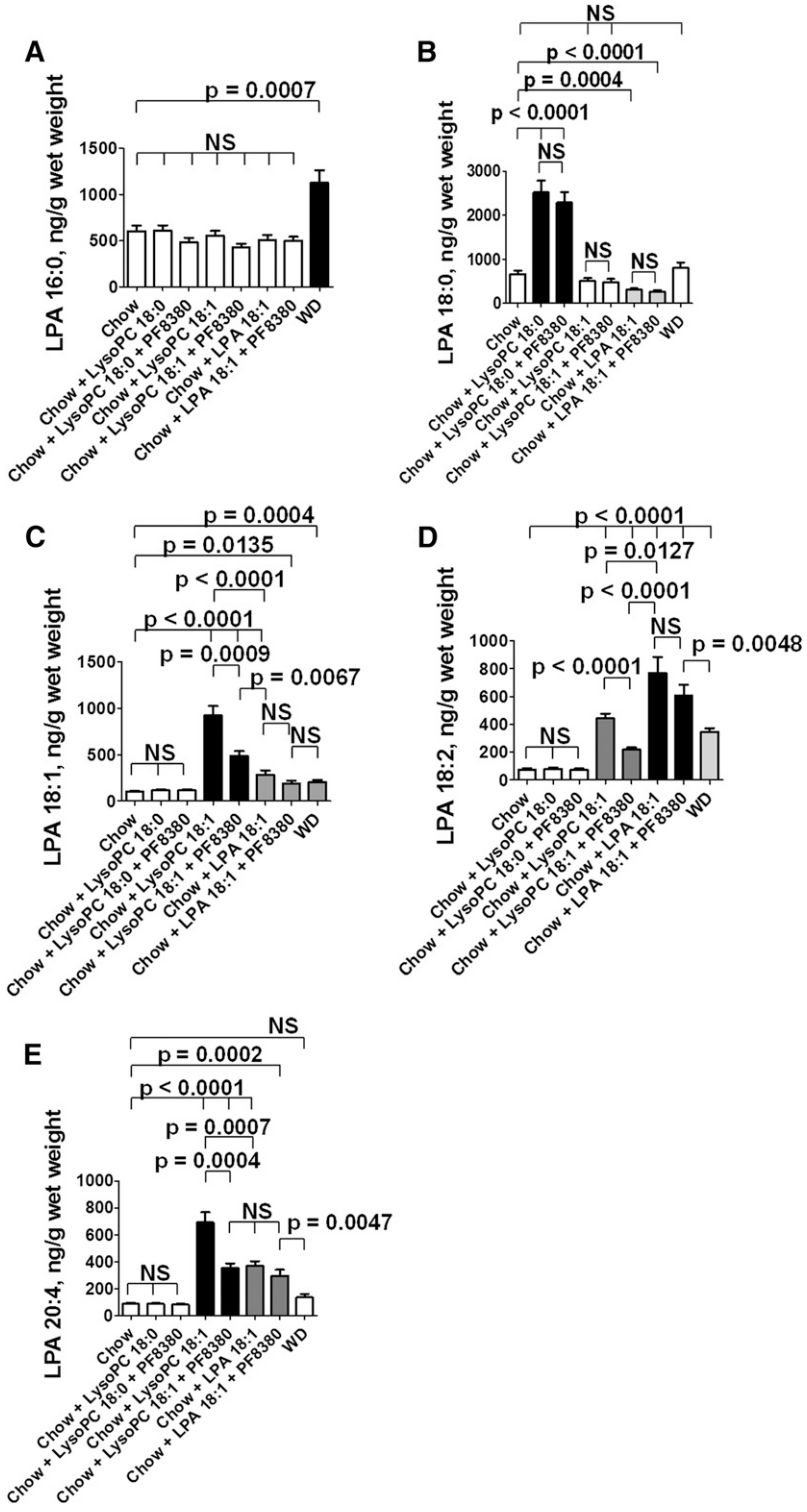

Fig. 9. Adding LysoPC 18:0 or LysoPC 18:1 or LPA 18:1 to standard mouse chow produces directional changes in the liver similar to those seen in the jejunum for most LPA species. After perfusion to remove all blood from the tissues, the liver was harvested from the mice described in Fig. 8, and hepatic LPA tissue levels were determined as described in Materials and Methods. A: The levels of LPA 16:0. B: The levels of LPA 18:0. C: The levels of LPA 18:1. D: The levels of LPA 18:2. E: The levels of LPA 20:4. The data shown are mean ± SEM. NS, not significant. If chow is included in multiple comparisons, each comparison is to chow.

higher levels in jejunum, liver, and plasma of LPA 18:1 and LPA 20:4 compared with adding LPA 18:1 to standard mouse chow. In contrast, adding LPA 18:1 to standard mouse chow resulted in higher levels in jejunum, liver, and plasma of LPA 18:2 compared with adding LysoPC 18:1 to standard mouse chow. In our previous publication, we reported that adding LPA 18:2 (but not LPA 18:0) to standard mouse chow did not increase the levels of LPA 18:0 in the tissue of the jejunum but significantly increased the levels of LPA 18:1 and 18:2 in the tissue of the jejunum (39). We also reported that adding LPA 18:2 (but not LPA 18:0) to standard mouse chow increased the levels of LPA 20:4 in the plasma (39). Our previous results and those reported here suggest that one of the responses to the feeding of these unsaturated lysophospholipids is a complex and robust remodeling of phospholipid fatty acids. There are multiple pathways for remodeling phospholipid fatty acids (52–56). We previously

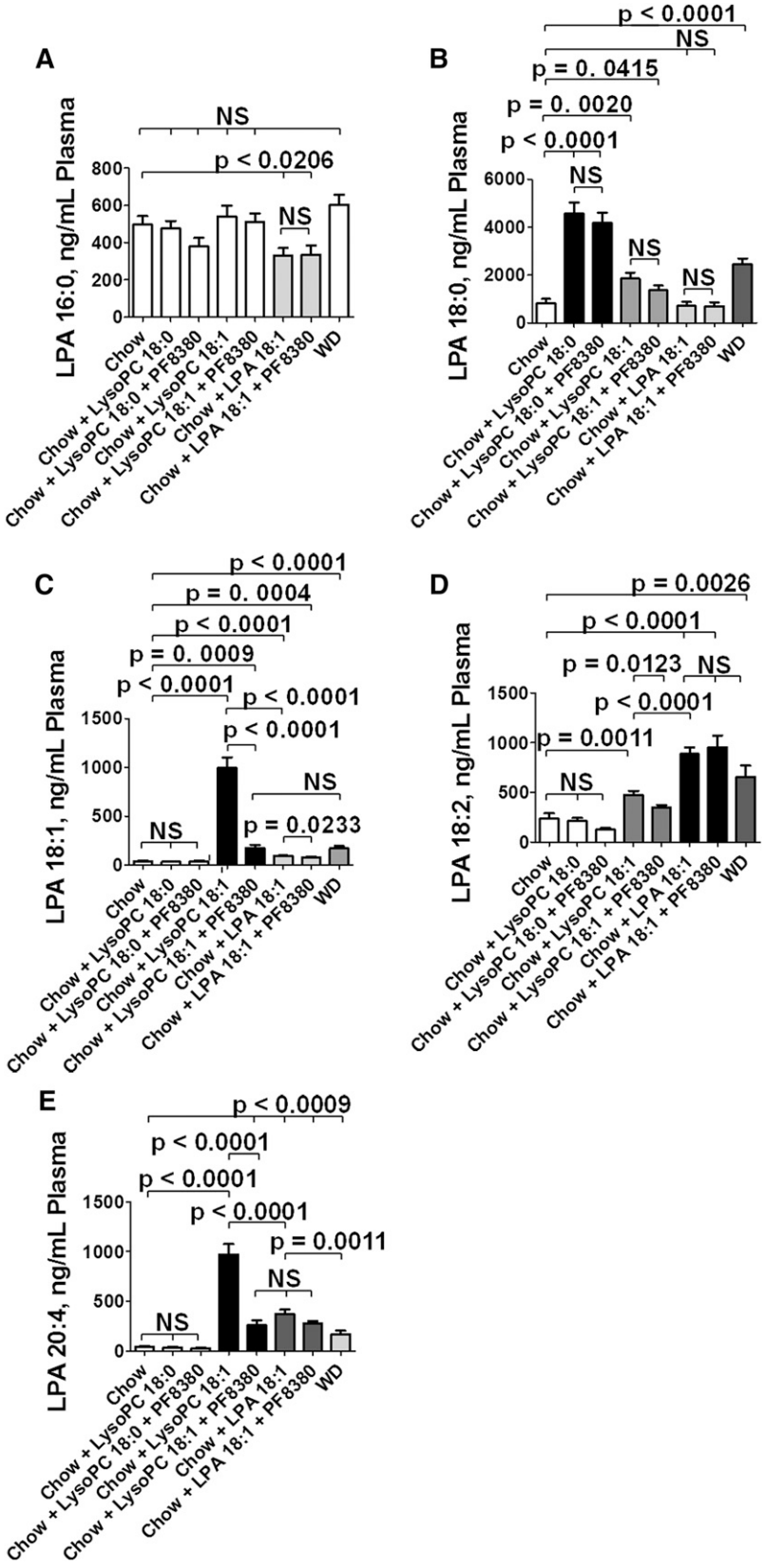

Fig. 10. Adding LysoPC 18:0 or LysoPC 18:1 or LPA 18:1 to standard mouse chow produces directional changes in the plasma similar to those seen in the jejunum and liver for most LPA species. Plasma LPA levels in the mice described in Fig. 8 were determined as described in Materials and Methods. A: The levels of LPA 16:0. B: The levels of LPA 18:0. C: The levels of LPA 18:1. D: The levels of LPA 18:2. E: The levels of LPA 20:4. The data shown are mean ± SEM. NS, not significant. If chow is included in multiple comparisons, each comparison is to chow.

reported that the expression of a number of genes known to be involved in fatty acid remodeling (*Acadl*, *Acot1*, *Acaa1b*, *Scd1*, and *Srebf1*) were significantly induced in the tissue of the jejunum when LPA 18:2 (but not LPA 18:0) was added to standard mouse chow (39). The significance of remodeling phospholipid fatty acids has recently been emphasized with the discovery of the role of lysophosphatidyl acyltransferase 3 (*Lpcat3*) (57). As shown in **Fig. 12**, adding LPA 18:2 (but not LPA 18:0) to standard mouse chow increased gene expression in the jejunum for

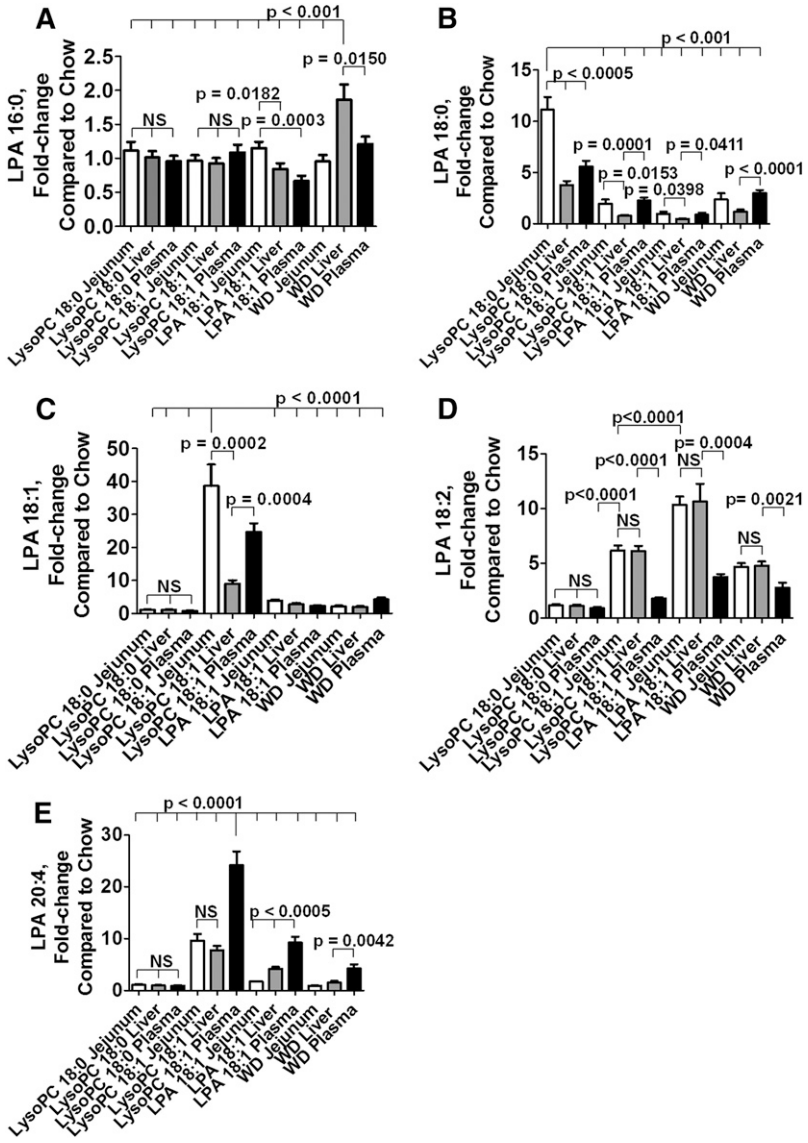

Fig. 11. Directly comparing changes in jejunum, liver, and plasma. An average value was calculated for each LPA species in each tissue in mice receiving standard chow without supplements in Figs. 8–10. The fold-change compared with the average value on standard mouse chow without supplements was then calculated for each mouse on each diet (except for those that received PF8380), and for each LPA species in the mice described in Figs. 8–10. In each panel, the fold-change in the jejunum compared with standard mouse chow without supplements is shown in white bars. In each panel the fold-change in the liver compared with standard mouse chow without supplements is shown in the gray bars. In each panel the fold-change in the plasma compared with standard mouse chow without supplements is shown in the black bars. Comparisons for mice receiving PF8380 were omitted to reduce the number of bars in each panel. A: The fold-change in levels of LPA 16:0. B: The fold-change in levels of LPA 18:0. C: The fold-change in levels of LPA 18:1. D: The fold-change in levels of LPA 18:2. E: The fold-change in levels of LPA 20:4. The data shown are mean ± SEM. NS, not significant. In the case of multiple comparisons, the index condition to which the others are compared is indicated by a long vertical line (e.g., in A, the multiple comparisons shown at the top of the figure were to the values for WD liver).

Lpcat3 to the same level as seen on feeding the LDLR$^{-/-}$ mice WD.

DISCUSSION

LPA 18:2-mediated dyslipidemia in LDLR$^{-/-}$ mice leads to aortic atherosclerosis

The results presented here (Fig. 1) confirm our previous finding that adding LPA 18:2 (but not LPA 18:0) to standard mouse chow causes dyslipidemia (39). Zhou et al. (26) reported that administration of ~1 μg of LPA 20:4 (but not LPA 18:0) by intraperitoneal injection in apoE null mice on a high-fat, high-cholesterol diet accelerated atherosclerosis without significantly altering the dyslipidemia. The data presented here demonstrate that addition of LPA 18:2 (but not LPA 18:0) to standard mouse chow causes dyslipidemia and aortic atherosclerosis in LDLR$^{-/-}$ mice similar to that seen on feeding the mice WD (Figs. 1–5). These results also demonstrate that both the dyslipidemia and aortic atherosclerosis were ameliorated by the addition of Tg6F tomatoes. Interestingly, the addition of the control tomatoes (EV tomatoes) to WD decreased the macrophage content of lesions (but not to the extent seen with Tg6F tomatoes) (Fig. 4). However, adding the control tomatoes to WD did not significantly change lesion area (Figs. 2 and 3), nor did it alter the content of α smooth muscle cell actin (Fig. 5).

Determining the source from which LPA 18:0 and LPA 18:1 are formed in the small intestine

Having confirmed our previous work (39), we sought to find a natural source of small intestine LPA other than the minimal levels of preformed LPA that are present in the diets (39). We previously reported that feeding LDLR$^{-/-}$ mice WD resulted in increased levels of unsaturated (but not saturated) LPA in the small intestine (39). Surprisingly, the content of preformed LPA in WD was actually lower than in standard mouse chow (39). The amount of

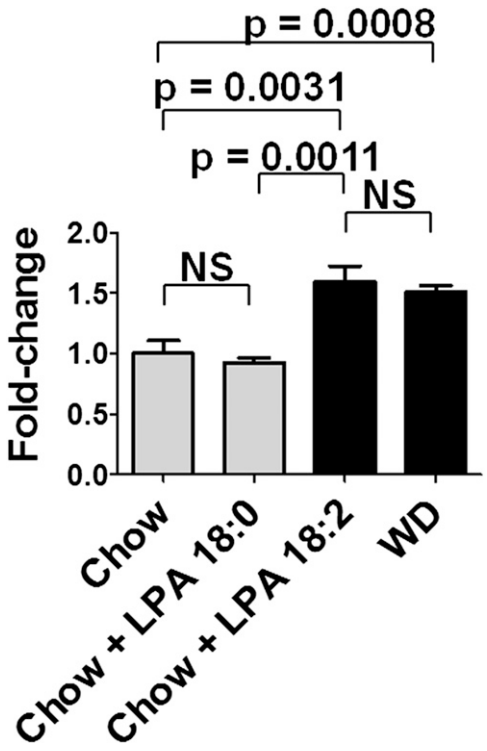

Fig. 12. Adding unsaturated (but not saturated LPA) to standard mouse chow induces gene expression of *Lpcat3* in the jejunum to the same level as seen after feeding the mice a WD. Female $LDLR^{-/-}$ mice age 7–8 months (7–8 per group) were fed standard mouse chow or standard mouse chow supplemented with 1 μg LPA 18:0 or LPA 18:2 per gram chow, or the mice were fed WD. After 2 weeks, the jejunum was harvested, and mRNA levels for *Lpcat3* were determined by RT-qPCR as described in Materials and Methods. The data shown are mean ± SEM. NS, not significant.

preformed LPA in either diet was only a very small fraction of the LPA 18:2 or LPA 18:0 added to standard mouse chow in our experiments, but the increase in the tissue of the small intestine of unsaturated LPA following the addition of LPA 18:2 was similar to that seen on feeding the mice WD. Feeding a high-fat diet is a potent stimulus for the production of PLA2G1B that acts to form LysoPC in the lumen of the proximal small intestine. The LysoPC is rapidly and efficiently taken up by the enterocytes of the small intestine (49). Autotaxin is known to be in abundance in the cells of the small intestine (51). Therefore, we hypothesized that a natural source of small intestine LPA would be LysoPC formed by the action of PLA2G1B in the lumen of the small intestine. PLA2G1B specifically removes the fatty acid from the *sn*-2 position of phospholipids, but it does not have specificity for the fatty acid removed from the *sn*-2 position (58).

In our previous studies, we used LPA 18:2 and LPA 18:0 with the fatty acids at the *sn*-1 position in each case (39). To test our hypothesis regarding PLA2G1B, we felt that we needed LysoPC and LPA with the same fatty acid at the same *sn*- position (e.g., LysoPC 18:0 with the 18:0 fatty acid at the *sn*-1 position and LPA 18:0 with the fatty acid at the *sn*-1 position, as well as LysoPC 18:1 with the 18:1 fatty acid at the *sn*-1 position and LPA 18:1 with the 18:1 fatty acid at the *sn*-1 position). These are all commercially available; in contrast, LysoPC 18:2 is not available, nor is LysoPC with the fatty acid at the *sn*-2 position. As described below, it is likely that the commercial availability of lysophospholipids with the acyl group at the *sn*-1 position is due to the relative stability of an acyl group at the *sn*-1 position and the difficulty in preventing isomerization from the *sn*-2 position to the *sn*-1 position of lysophospholipids. Consequently, we used LysoPC 18:0, LysoPC 18:1, and LPA 18:1 all with the fatty acid at the *sn*-1 position for these experiments. It should be noted that our previous work demonstrated that when phosphatidic acid with the same fatty acid at both the *sn*-1 and *sn*-2 positions (i.e., 18:0 or 18:2 at both positions) was added to normal mouse chow, similar results were obtained compared with adding LPA 18:0 or LPA 18:2 with the fatty acid at the *sn*-1 position (39).

Because most phospholipids contain a saturated fatty acid at the *sn*-1 position and an unsaturated fatty acid at the *sn*-2 position, it would not be unreasonable to ask if using phospholipid species with the unsaturated fatty acid at the *sn*-1 position is relevant. If one considers the distribution of 18:1 fatty acids in phospholipids at the *sn*-1 position versus the *sn*-2 position, 15% of the 18:1 fatty acids in phospholipids are found at the *sn*-1 position in chicken eggs (59). In bovine brain, 30% of the 18:1 fatty acids in phospholipids are found at the *sn*-1 position (59). In human erythrocytes and in human plasma, the values are 17% and 21%, respectively (59). In rat lung, heart, and liver 37%, 35%, and 35% of the 18:1 fatty acids in phospholipids are found at the *sn*-1 position, respectively (59). Thus, while it is more likely that the *sn*-1 position will contain a saturated fatty acid, it is certainly not rare to find an unsaturated fatty acid at the *sn*-1 position. The data presented here show that the unsaturated species that we chose were biologically active. While we can be confident of the *sn*- position of the phospholipids added to standard mouse chow (i.e., the acyl group was at the *sn*-1 position), isomerization of acyl groups in phospholipids is common, particularly movement of the acyl group from the *sn*-2 to the *sn*-1 position in cases where the *sn*-1 position initially does not have an acyl group (60, 61). The *sn*-1 position appears to be more thermodynamically stable for accommodating an acyl group in lysophospholipids than is the case at the *sn*-2 position (60, 61). The method that we used to measure LPA species in jejunum, liver, and plasma (LC/MS/MS) does not allow us to determine which *sn*- position is occupied by the acyl group.

We chose to use PF8380 to test our hypothesis because it has been shown to be highly specific in inhibiting autotaxin activity (42) and effective at the dose used in the experiments described here (30 mg/kg) (42, 43). Moreover, PF8380 has been shown both in vitro and in vivo to have the ability to block the autotaxin-mediated conversion of LysoPC 18:0 to LPA 18:0 as well as being able to block the autotaxin-mediated conversion of LysoPC 18:1 to LPA 18:1 (42). As shown in Figs. 8–10, adding LysoPC 18:0 to standard mouse chow resulted in a marked increase in the levels of LPA 18:0 in jejunum, liver, and plasma, but

the increase was not significantly ameliorated by PF8380. These data are consistent with LysoPC 18:0 being converted to LPA 18:0 by autotaxin-independent pathways.

One might wonder if autotaxin could have a preference for unsaturated LysoPC, and if the failure of PF8380 to block the conversion of LysoPC 18:0 to LPA 18:0 might be due to the specificity of autotaxin. There is one report in the literature suggesting that autotaxin may be modestly more active in converting LysoPC 18:1 to LPA 18:1 compared with the conversion of LysoPC 18:0 to LPA 18:0 (62). However, two other studies reported that autotaxin was equally effective in converting LysoPC 18:0 to LPA 18:0 as compared with the conversion of LysoPC 18:1 to LPA 18:1 (42, 63). Thus, it seems more likely that the failure of PF8380 to alter the conversion of LysoPC 18:0 to LPA 18:0 was due to the processing of LysoPC 18:0 by an autotaxin-independent pathway in our experiments. We must assume that the conversion of LysoPC 18:0 to LPA 18:0 in our mice occurred in a microenvironment devoid of autotaxin, or there must be another enzyme(s) present with much higher affinity for the substrate (LysoPC 18:0) compared with autotaxin. Our data do not shed any light on this issue, and the details of these processes must be determined by future research. Regardless of how LysoPC 18:0 is converted to LPA 18:0 our data clearly demonstrate that the resulting increased levels of LPA 18:0 are not associated with dyslipidemia and inflammation, as is the case for LPA 18:1, LPA 18:2, and LPA 20:4.

Our LC/MS/MS data are highly consistent with LysoPC 18:1 being converted to LPA 18:1 by an autotaxin-dependent mechanism (i.e., the levels of LPA 18:1 after feeding LysoPC 18:1 were significantly reduced in all tissues by PF8380). Moreover, the LysoPC 18:1-mediated changes in plasma levels of total cholesterol, triglycerides, HDL-cholesterol, and PON activity were all significantly ameliorated by PF8380 (Fig. 7A–D).

In these studies, we did not directly test if the dyslipidemia caused by feeding LysoPC 18:1 would cause atherosclerosis, as was the case for LPA 18:2. However, it was recently reported that $LDLR^{-/-}$ mice that were also deficient in PLA2G1B had a dramatic reduction in aortic atherosclerosis (50), which would be consistent with the LysoPC-mediated dyslipidemia causing atherosclerosis.

The results with PF8380 strongly implicate autotaxin in the processing of unsaturated LysoPC 18:1 to unsaturated LPA species (Figs. 8–10), which cause dyslipidemia (Fig. 7). However, these findings are not definitive. Definitive proof that dietary unsaturated LysoPC must be converted to unsaturated LPA in the small intestine by an autotaxin-dependent mechanism in order to cause dyslipidemia and atherosclerosis will require an intestinal specific knockout of autotaxin. We are currently breeding such mice.

There are complex and robust mechanisms for remodeling phospholipid fatty acids

We previously reported (39) that adding one species of unsaturated LPA to chow resulted in a significant increase in the species added but also resulted in a significant increase in other unsaturated species of LPA. These findings suggest that the unsaturated LPA added to standard mouse chow may be taken up by enterocytes and stimulate the formation of other species of unsaturated LPA and perhaps may also stimulate the formation of the same species of LPA in the enterocytes. The pathways for the formation, degradation, and recycling of LPA are complex (23–25, 52–56), and it is therefore not surprising that inhibiting autotaxin might have some effect on the actions of unsaturated LPA added to standard mouse chow. The important role of *Lpcat3* in maintaining a diversity of phospholipid fatty acids by favoring the formation of phospholipids with unsaturated fatty acids has recently been highlighted (57). As shown in Fig. 12, the increase in gene expression in the jejunum of *Lpcat3* after adding LPA 18:2 (but not LPA 18:0) to standard mouse chow was similar to that seen on feeding the mice WD.

The responses to LysoPC and LPA are complex

In jejunum, liver, and plasma the greatest increase in levels of LPA 18:1 was seen after adding LysoPC 18:1 to standard mouse chow, not after adding LPA 18:1 (Figs. 8C, 9C, and 10C). In contrast, the greatest increase in levels of LPA 18:2 was seen in jejunum, liver, and plasma after adding LPA 18:1 to standard mouse chow compared with adding LysoPC 18:1 (Figs. 8D, 9D, and 10D). The greatest increase in levels of LPA 20:4 was seen in jejunum, liver, and plasma after adding LysoPC 18:1 to standard mouse chow compared with adding LPA 18:1 (Figs. 8E, 9E, and 10E).

Because linoleic acid (18:2) is an essential fatty acid (i.e., it cannot be synthesized de novo in mammalian cells), it is likely that the increase in LPA 18:2 after adding LPA 18:1 to standard mouse chow involves acyltransferase activity. It is known that *Lpcat3* preferentially uses linoleic acid (57). *Lpcat3* gene expression in the jejunum was increased after adding LPA 18:2 to standard mouse chow (Fig. 12). Assuming Lpcat3 activity in the jejunum would similarly increase after adding LPA 18:1, the increase in LPA 18:2 could have been due to *Lpcat3*-mediated production of more phospholipids containing linoleic acid, which were then converted to LPA 18:2. Thus, the tissue response to intestine-derived lysophospholipids is very complex. The identification of the mechanisms responsible for this complexity awaits future research.

Possible mechanisms by which unsaturated LPA may promote dyslipidemia and apoA-I mimetic peptides may ameliorate dyslipidemia

The mechanisms by which unsaturated (but not saturated) LPA mediates dyslipidemia and atherosclerosis (Figs. 1–5), and the mechanisms by which Tg6F tomatoes inhibit this process (Figs. 1–5) are unknown. One potential mechanism might involve the balance between inositol-requiring enzyme 1 (*Ire1*) and microsomal triglyceride transfer protein (*Mtp*). The *Ire1* genes are involved in sensing and modulating endoplasmic reticulum stress (64, 65). *Ire1α* is expressed in all mammalian cells, but *Ire1β* is expressed primarily in intestinal epithelial cells (66).

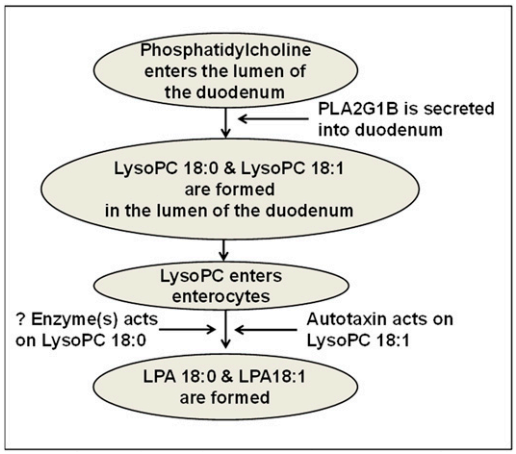

Fig. 13. A schematic representation of the formation of LPA 18:0 and LPA 18:1 in the small intestine. It is hypothesized that phosphatidylcholine in the lumen of the small intestine is acted on by pancreatic PLA2G1B to produce saturated LysoPC (e.g., LysoPC 18:0) or unsaturated LysoPC (e.g., LysoPC 18:1) in the lumen of the small intestine. The resulting LysoPC enters the enterocytes of the small intestine where the saturated LysoPC is converted to saturated LPA (e.g., LPA 18:0) by unknown (?) enzyme(s), while unsaturated LysoPC is converted to unsaturated LPA (e.g., LPA 18:1) by lysophospholipase D (autotaxin).

Wild-type mice fed WD compared with chow showed decreased mRNA levels of *Ire1β* and increased levels of mRNA for *Mtp* in intestinal tissue (67). Mice null for *Ire1β* when fed WD developed more pronounced hyperlipidemia compared with wild-type mice because the *Ire1β* null mice secreted more chylomicrons and expressed more intestinal MTP, but not more hepatic MTP (67). Cell culture studies showed that *Ire1β* (but not *Ire1α*) decreased *Mtp* RNA through increased posttranscriptional degradation; and conversely, knockdown of *Ire1β* enhanced *Mtp* expression in the cells (67). In a subsequent study, it was shown that mice null for apoE that were also null for *Ire1β* had higher levels of intestinal MTP (but not apoB), absorbed more lipids because of enhanced secretion of intestinal chylomicrons, and exhibited greater hyperlipidemia due to an increased number of apoB-containing remnant lipoproteins (with no significant change in composition) compared with apoE null mice that were wild-type for *Ire1β* (68). The increased plasma lipids in the double knockout mice were not due to changes in hepatic lipoprotein production. The double knockout mice also had greater aortic atherosclerosis on both chow and WD (68). These studies suggest that this pathway might be a fruitful line of investigation for future studies.

The recent publication by Zhao et al. (69) showing that an apoA-I mimetic peptide structurally different from the 4F and 6F peptides was effective after oral administration despite the absence of detectable plasma levels strongly suggests that the site of action for multiple apoA-I mimetic peptides may be in the gut (69, 70). The results reported here suggest that studying the role of apoA-I mimetic peptides in LysoPC metabolism in the small intestine may be a fruitful line of research.

SUMMARY

The data reported here suggest that dietary unsaturated LysoPC may be converted to unsaturated LPA by an autotaxin-dependent mechanism in the enterocytes of the small intestine and lead to dyslipidemia and atherosclerosis in LDLR$^{-/-}$ mice. The conversion of diet-derived saturated LysoPC to saturated LPA appears to readily occur, but by an autotaxin-independent process. A schematic diagram of these processes is shown in **Fig. 13**. Finding the different mechanisms involved in processing diet-derived saturated LysoPC compared with those involved in processing diet-derived unsaturated LysoPC, and determining why the former does not lead to dyslipidemia while the latter does, is likely to provide important new insights into lipid and lipoprotein metabolism. The data presented here together with our previously published data (11, 39) point to the small intestine as an increasingly interesting potential target for the management of dyslipidemia and atherosclerosis.

REFERENCES

1. Reddy, S. T., M. Navab, G. M. Anantharamaiah, and A. M. Fogelman. 2014. Searching for a successful HDL-based treatment strategy. *Biochim. Biophys. Acta.* **1841:** 162–167.
2. Navab, M., I. Shechter, G. M. Anantharamaiah, S. T. Reddy, B. J. Van Lenten, and A. M. Fogelman. 2010. Structure and function of HDL mimetics. *Arterioscler. Thromb. Vasc. Biol.* **30:** 164–168.
3. Bloedon, L. T., R. Dunbar, D. Duffy, P. Pinell-Salles, R. Norris, B. J. DeGroot, R. Movva, M. Navab, A. M. Fogelman, and D. J. Rader. 2008. Safety, pharmacokinetics, and pharmacodynamics of oral apoA-I mimetic peptide D-4F in high-risk cardiovascular patients. *J. Lipid Res.* **49:** 1344–1352.
4. Dunbar, R.L., L.T. Bloedon, D. Duffy, R.B. Norris, R. Movva, M. Navab, A.M. Fogelman, and D.J. Rader 2007. Daily oral administration of the apolipoprotein A-I mimetic peptide D-4F in patients with coronary heart disease or equivalent risk improves high-density lipoprotein anti-inflammatory function (Abstract). *J. Am. Coll. Cardiol.* **49:** 366A.
5. Watson, C. E., N. Weissbach, L. Kjems, S. Ayalasomayajula, Y. Zhang, I. Chang, M. Navab, S. Hama, G. Hough, S. T. Reddy, et al. 2011. Treatment of patients with cardiovascular disease with L-4F, an apoA-1 mimetic, did not improve select biomarkers of HDL function. *J. Lipid Res.* **52:** 361–373.
6. Navab, M., S. T. Reddy, G. M. Anantharamaiah, S. Imaizumi, G. Hough, S. Hama, and A. M. Fogelman. 2011. Intestine may be a major site of action for the apoA-I mimetic peptide 4F whether administered subcutaneously or orally. *J. Lipid Res.* **52:** 1200–1210.
7. Navab, M., S. T. Reddy, G. M. Anantharamaiah, G. Hough, G. M. Buga, J. Danciger, and A. M. Fogelman. 2012. D-4F-mediated reduction in metabolites of arachidonic and linoleic acids in the small intestine is associated with decreased inflammation in low-density lipoprotein receptor-null mice. *J. Lipid Res.* **53:** 437–445.
8. Van Lenten, B. J., A. C. Wagner, M. Navab, G. M. Anantharamaiah, S. Hama, S. T. Reddy, and A. M. Fogelman. 2007. Lipoprotein inflammatory properties and serum amyloid A levels but not cholesterol levels predict lesion area in cholesterol-fed rabbits. *J. Lipid Res.* **48:** 2344–2353.
9. Navab, M., G. M. Anantharamaiah, S. T. Reddy, B. J. Van Lenten, B. J. Ansell, G. C. Fonarow, K. Vahabzadeh, S. Hama, G. Hough, N. Kamranpour, et al. 2004. The oxidation hypothesis of atherogenesis: the role of oxidized phospholipids and HDL. *J. Lipid Res.* **45:** 993–1007.
10. Navab, M., G. M. Anantharamaiah, S. Hama, G. Hough, S. T. Reddy, J. S. Frank, D. W. Garber, S. Handattu, and A. M. Fogelman. 2005. D-4F and statins synergize to render HDL anti-inflammatory in mice and monkeys and cause lesion regression in old apolipoprotein E-null mice. *Arterioscler. Thromb. Vasc. Biol.* **25:** 1426–1432.

11. Chattopadhyay, A., M. Navab, G. Hough, F. Gao, D. Meriwether, V. Grijalva, J. R. Springstead, M. N. Palgunachari, R. Namiri-Kalantari, F. Su, et al. 2013. A novel approach to oral apoA-I mimetic therapy. *J. Lipid Res.* **54:** 995–1010. [Erratum. 2013. *J. Lipid Res.* 54: 3220.]
12. Panchatcharam, M., A. K. Salous, J. Brandon, S. Miriyala, J. Wheeler, P. Patil, M. Sunkara, A. J. Morris, D. Escalante-Alcadle, and S. S. Smyth. 2014. Mice with targeted inactivation of Ppap2b in endothelial and hematopoietic cells display enhanced vascular inflammation and permeability. *Arterioscler. Thromb. Vasc. Biol.* **34:** 837–845.
13. Lin, M-E., D. R. Herr, and J. Chun. 2010. Lysophosphatidic acid (LPA) receptors: signaling properties and disease relevance. *Prostaglandins Other Lipid Mediat.* **91:** 130–138.
14. Xiang, S. Y., S. S. Dusaban, and J. H. Brown. 2013. Lysophospholipid receptor activation of RhoA and lipid signaling pathways. *Biochim. Biophys. Acta.* **1831:** 213–222.
15. Ueda, H., H. Matsunaga, O. I. Olaposi, and J. Nagai. 2013. Lysophosphatidic acid: chemical signature of neuropathic pain. *Biochim. Biophys. Acta.* **1831:** 61–73.
16. Ren, H., M. Panchatcharam, P. Mueller, D. Escalante-Alcalde, A. J. Morris, and S. S. Smyth. 2013. Lipid phosphate phosphatase (LPP3) and vascular development. *Biochim. Biophys. Acta.* **1831:** 126–132.
17. Peyruchaud, O., R. Leblanc, and M. David. 2013. Pleiotropic activity of lysophosphatidic acid in bone metastasis. *Biochim. Biophys. Acta.* **1831:** 99–104.
18. Mansell, J. P., and J. Blackburn. 2013. Lysophosphatidic acid, human osteoblast formation, maturation and the role of 1α,25-Dihydroxyvitamin D3 (calcitriol). *Biochim. Biophys. Acta.* **1831:** 105–108.
19. Sims, S. M., N. Panupinthu, D. M. Lapierre, A. Pereverev, and S. J. Dixon. 2013. Lysophosphatidic acid: a potential mediator of osteoblast-osteoclast signaling in bone. *Biochim. Biophys. Acta.* **1831:** 109–116.
20. Sevastou, I., E. Kaffe, M. A. Mouratis, and V. Aidinis. 2013. Lysoglycerophospholipids in chronic inflammatory disorders: the PLA(2)/LPC and ATX/LPA axes. *Biochim. Biophys. Acta.* **1831:** 42–60.
21. Choi, J. W., and J. Chun. 2013. Lysophospholipids and their receptors in the central nervous system. *Biochim. Biophys. Acta.* **1831:** 20–32.
22. Yanagida, K., Y. Kurikawa, T. Shimizu, and S. Ishii. 2013. Current progress in non-Edg family LPA receptor research. *Biochim. Biophys. Acta.* **1831:** 33–41.
23. Aoki, J., A. Inoue, and S. Okudaira. 2008. Two pathways for lysophosphatidic acid production. *Biochim. Biophys. Acta.* **1781:** 513–518.
24. Mills, G. B., and W. H. Moolenaar. 2003. The emerging role of lysophosphatidic acid in cancer. *Nat. Rev. Cancer.* **3:** 582–591.
25. Brindley, D. N., and C. Pilquil. 2009. Lipid phosphate phosphatases and signaling. *J. Lipid Res.* **50:** S225–S230.
26. Zhou, Z., P. Subramanian, G. Sevilmis, B. Globke, O. Soehnlein, E. Karshovska, R. Megens, K. Heyll, J. Chun, J. S. Saulnier-Blache, et al. 2011. Lipoprotein-derived lysophosphatidic acid promotes atherosclerosis by releasing CXCL1 from the endothelium. *Cell Metab.* **13:** 592–600.
27. Panchatcharam, M., S. Miriyala, A. Salous, J. Wheeler, A. Dong, P. Mueller, M. Sunkara, D. Escalante-Alcalde, A. J. Morris, and S. S. Smyth. 2013. Lipid phosphate phosphatase 3 negatively regulates smooth muscle cell phenotypic modulation to limit intimal hyperplasia. *Arterioscler. Thromb. Vasc. Biol.* **33:** 52–59.
28. Schunkert, H., I. R. König, S. Kathiresan, et al.; CARDIoGRAM Consortium. 2011. Large-scale association analysis identifies 13 new susceptibility loci for coronary artery disease. *Nat. Genet.* **43:** 333–338.
29. Rai, V., F. Toure, S. Chitayat, R. Pei, F. Song, Q. Li, J. Zhang, R. Rosario, R. Ramasamy, W. J. Chazin, et al. 2012. Lysophosphatidic acid targets vascular and oncogenic pathways via RAGE signaling. *J. Exp. Med.* **209:** 2339–2350.
30. Schober, A., and W. Siess. 2012. Lysophosphatidic acid in atherosclerotic diseases. *Br. J. Pharmacol.* **167:** 465–482.
31. Shen, X., W. Wang, L. Wang, C. Houde, W. Wu, M. Tudor, J. R. Thompson, C. M. Sisk, B. Hubbard, and J. Li. 2012. Identification of genes affecting apolipoprotein B secretion following siRNA-mediated gene knockdown in primary human hepatocytes. *Atherosclerosis.* **222:** 154–157.
32. Dohi, T., K. Miyauchi, R. Ohkawa, K. Nakamura, M. Kurano, T. Kishimoto, N. Yanagisawa, M. Ogita, T. Miyazaki, A. Nishino, et al. 2013. Increased lysophosphatidic acid levels in culprit coronary arteries of patients with acute coronary syndrome. *Atherosclerosis.* **229:** 192–197.
33. Natarajan, V., W. M. Scribner, C. M. Hart, and S. Parthasarathy. 1995. Oxidized low density lipoprotein-mediated activation of phospholipase D in smooth muscle cells: a possible role in cell proliferation and atherogenesis. *J. Lipid Res.* **36:** 2005–2016.
34. Chen, C., L. N. Ochoa, A. Kagan, H. Chai, Z. Liang, P. H. Lin, and Z. Yao. 2012. Lysophosphatidic acid causes endothelial dysfunction in porcine coronary arteries and human coronary artery endothelial cells. *Atherosclerosis.* **222:** 74–83.
35. Llordá, J., V. Angeli, J. Liu, E. Trogan, E. A. Fisher, and G. J. Randolph. 2004. Emigration of monocyte-derived cells from atherosclerotic lesions characterizes regressive, but not progressive, plaques. *Proc. Natl. Acad. Sci. USA.* **101:** 11779–11784.
36. Bot, M., I. Bot, R. Lopez-Vales, C. H. A. van de Lest, J. S. Saulnier-Blache, J. B. Helms, S. David, T. J. C. van Berkel, and E. A. L. Biessen. 2010. Atherosclerotic lesion progression changes lysophosphatidic acid homeostasis to favor its accumulation. *Am. J. Pathol.* **176:** 3073–3084.
37. Bot, M., S. C. A. de Jager, L. MacAleese, H. M. Lagraauw, T. J. C. van Berkel, P. H. A. Quax, J. Kuiper, R. M. A. Heeren, E. A. L. Biessen, and I. Bot. 2013. Lysophosphatidic acid triggers mast cell-driven atherosclerotic plaque destabilization by increasing vascular inflammation. *J. Lipid Res.* **54:** 1265–1274.
38. Smyth, S. S., P. Mueller, F. Yang, J. A. Brandon, and A. J. Morris. 2014. Arguing the case for the autotaxin-lysophosphatidic acid-lipid phosphate phosphatase 3-signaling nexus in the development and complications of atherosclerosis. *Arterioscler. Thromb. Vasc. Biol.* **34:** 479–486.
39. Navab, M., G. Hough, G. M. Buga, F. Su, A. C. Wagner, D. Meriwether, A. Chattopadhyay, F. Gao, V. Grijalva, J. S. Danciger, et al. 2013. Transgenic 6F tomatoes act on the small intestine to prevent systemic inflammation and dyslipidemia caused by Western diet and intestinally derived lysophosphatidic acid. *J. Lipid Res.* **54:** 3403–3418.
40. Remaley, A. T. 2013. Tomatoes, lysophosphatidic acid and the small intestine: new pieces in the puzzle of apolipoprotein mimetic peptides? *J. Lipid Res.* **54:** 3223–3226.
41. Kok, B. P., G. Venkatraman, D. Capatos, and D. N. Brindley. 2012. Unlike two peas in a pod: lipid phosphate phosphatases and phosphatidate phosphatases. *Chem. Rev.* **112:** 5121–5146.
42. Gierse, J., A. Thorarensen, K. Beltey, E. Brandshaw-Pierce, L. Cortes-Burgos, T. Hall, A. Johnston, M. Murphy, O. Nemirovskiy, S. Ogawa, et al. 2010. A novel autotaxin inhibitor reduces lysophosphatidic acid levels in plasma and the site of inflammation. *J. Pharmacol. Exp. Ther.* **334:** 310–317.
43. Salous, A. K., M. Panchatcharam, M. Sunkara, P. Mueller, A. Dong, Y. Wang, G. A. Graf, S. S. Smyth, and A. J. Morris. 2013. Mechanism of rapid elimination of lysophosphatidic acid and related lipids from the circulation of mice. *J. Lipid Res.* **54:** 2775–2784.
44. Navab, M., S. Hama, G. Hough, and A. M. Fogelman. 2003. Oral synthetic phospholipid (DMPC) raises high-density lipoprotein cholesterol levels, improves high-density lipoprotein function, and markedly reduces atherosclerosis in apolipoprotein E-null mice. *Circulation.* **108:** 1735–1739.
45. Huggins, K. W., A. C. Boileau, and D. Y. Hui. 2002. Protection against diet-induced obesity and obesity-related insulin resistance in Group 1B PLA_2-deficient mice. *Am. J. Physiol. Endocrinol. Metab.* **283:** E994–E1001.
46. Labonté, E. D., R. J. Kirby, N. M. Schildmeyer, A. M. Cannon, K. W. Huggins, and D. Y. Hui. 2006. Group 1B phospholipase A_2-mediated lysophospholipid absorption directly contributes to postprandial hyperglycemia. *Diabetes.* **55:** 935–941.
47. Labonté, E. D., P. T. Pfluger, J. G. Cash, D. G. Kuhel, J. C. Roja, D. P. Magness, R. J. Jandacek, H. Tschop, and D. Y. Hui. 2010. Postprandial lysophospholipid suppresses hepatic fatty acid oxidation: the molecular link between group 1B phospholipase A2 and diet-induced obesity. *FASEB J.* **24:** 2516–2524.
48. Hollie, N. I., and D. Y. Hui. 2011. Group 1B phospholipase A2 deficiency protects against diet-induced hyperlipidemia in mice. *J. Lipid Res.* **52:** 2005–2011.
49. Hui, D. Y. 2012. Phospholipase A2 enzymes in metabolic and cardiovascular diseases. *Curr. Opin. Lipidol.* **23:** 235–240.
50. Hollie, N. I., E. S. Konaniah, C. Goodin, and D. Y. Hui. 2014. Group 1B phospholipase A2 inactivation suppresses atherosclerosis and metabolic diseases in LDL receptor-deficient mice. *Atherosclerosis.* **234:** 377–380.
51. Lee, H. Y., J. Murata, T. Clair, M. H. Polymeropoulos, R. Torres, R. E. Manrow, L. A. Liotta, and M. L. Stracke. 1996. Cloning,

chromosomal localization, and tissue expression of autotaxin from human teratocarcinoma cells. *Biochem. Biophys. Res. Commun.* **218:** 714–719.
52. Sugiura, T., Y. Masuzawa, and K. Waku. 1988. Coenzyme A-dependent transacylation system in rabbit liver microsomes. *J. Biol. Chem.* **263:** 17490–17498.
53. Yamashita, A., T. Sugiura, and K. Waku. 1997. Acytransferases and transacylases involved in fatty acid remodeling of phospholipids and metabolism of bioactive lipids in mammalian cells. *J. Biochem.* **122:** 1–16.
54. Gossett, R. E., R. D. Edmondson, C. A. Jolly, T-H. Cho, D. H. Russell, J. Knudsen, A. B. Kier, and F. Schroeder. 1998. Structure and function of normal and transformed murine acyl-coA binding proteins. *Arch. Biochem. Biophys.* **350:** 201–213.
55. Jolly, C. A., D. C. Wilton, and F. Schroeder. 2000. Microsomal fatty acyl-CoA transacylation and hydrolysis: fatty acyl-CoA species dependent modulation by liver fatty acyl-CoA binding proteins. *Biochim. Biophys. Acta.* **1483:** 185–197.
56. Yamashita, A., N. Kawagishi, T. Miyashita, T. Nagatsuka, T. Sugiura, K. Kume, T. Shimizu, and K. Waku. 2001. ATP-independent fatty acyl-coenzyme A synthesis from phospholipid: coenzyme A-dependent transacylation activity toward lysophosphatidic acid catalyzed by acyl-coenzyme A:lyosphosphatic acyltransferase. *J. Biol. Chem.* **276:** 26745–26752.
57. Rong, X., C. J. Albert, C. Hong, M. A. Duerr, B. T. Chamberlain, E. J. Tarling, A. Ito, J. Gao, B. Wang, P. A. Edwards, et al. 2013. LXRs regulate ER stress and inflammation through dynamic modulation of membrane phospholipid composition. *Cell Metab.* **18:** 685–697.
58. Snitko, Y., S. K. Han, B. I. Lee, and W. Cho. 1999. Differential interfacial and substrate binding modes of mammalian pancreatic phospholipases A2: a comparison among human, bovine, and porcine enzymes. *Biochemistry.* **38:** 7803–7810.
59. Christie, W. W. 2014. Phosphatidylcholine and related lipids; structure, occurrence, biochemistry and analysis. The AOCS Lipid Library. Accessed January 7, 2015, at http://lipidlibrary.aocs.org/Lipids/pc/index.htm.
60. Adlercreutz, D., H. Budde, and E. Wehtje. 2002. Synthesis of phosphatidylcholine with defined fatty acid in the sn-1 position by lipase-catalyzed esterification and transesterification reaction. *Biotechnol. Bioeng.* **78:** 403–411.
61. D'Arrigo, P., and S. Servi. 2010. Synthesis of lysophospholipids. *Molecules.* **15:** 1354–1377.
62. Tokumura, A., E. Majima, Y. Kariya, K. Tominaga, K. Kogure, K. Yasuda, and K. Fukuzawa. 2002. Identification of human plasma lysophospholipase D, a lysophosphatidic acid-producing enzyme, as autotaxin, a multifunctional phosphodiesterase. *J. Biol. Chem.* **277:** 39436–39442.
63. Giganti, A., M. Rodriguez, B. Fould, N. Moulharat, F. Coge, P. Chomarat, J-P. Galizzi, P. Valet, J-S. Saulnier-Blache, J. A. Boutin, et al. 2008. Murine and human autotaxin α, β, and γ isoforms: gene organization, tissue distribution, and biochemical characterization. *J. Biol. Chem.* **283:** 7776–7789.
64. Bernales, S., F. R. Papa, and P. Walter. 2006. Intracellular signaling by the unfolded protein response. *Annu. Rev. Cell Dev. Biol.* **22:** 487–508.
65. Bertolotti, A., Y. Zhang, L. M. Hendershot, H. P. Harding, and D. Ron. 2000. Dynamic interaction of BiP and ER stress transducers in the unfolded-protein response. *Nat. Cell Biol.* **2:** 326–332.
66. Bertolotti, A., X. Wang, I. Novoa, R. Jungreis, K. Schlessinger, J. H. Chow, A. B. West, and D. Ron. 2001. Increased sensitivity to dextran sodium sulfate colitis in IRE1beta-deficient mice. *J. Clin. Invest.* **107:** 585–593.
67. Iqbal, J., K. Dai, T. Seimon, R. Jungreis, M. Oyadomari, G. Kuriakose, D. Ron, I. Tabas, and M. M. Hussain. 2008. IRE1β inhibits chylomicron production by selectively degrading MTP mRNA. *Cell Metab.* **7:** 445–455.
68. Iqbal, J., J. Queiroz, Y. Li, X-C. Jiang, D. Ron, and M. M. Hussain. 2012. Increased intestinal lipid absorption caused by Ire1β deficiency contributes to hyperlipidemia and atherosclerosis in apolipoprotein E-deficient mice. *Circ. Res.* **110:** 1575–1584.
69. Zhao, Y., A. S. Black, D. J. Bonnet, B. E. Maryanoff, L. K. Curtiss, L. J. Leman, and M. R. Ghadiri. 2014. In vivo efficacy of HDL-like nanolipid particles containing multivalent peptide mimetics of apolipoprotein A-I. *J. Lipid Res.* **55:** 2053–2063.
70. Wool, G. D., C. A. Reardon, and G. S. Getz. 2014. Mimetic peptides of human apoA-I helix 10 gets together to lower lipids and ameliorate atherosclerosis: Is the action in the gut? *J. Lipid Res.* **55:** 1983–1985.